4-2015

Early Miocene Antarctic glacial history: New insights from heavy mineral analysis from ANDRILL AND–2A drill core sediments

Francesco Iacoviello
University College London, iacoviello.francesco@gmail.com

Giovanna Giorgetti
Università di Siena, giorgettig@unisi.it

Isabella Turbanti Memmi
Università degli Studi di Siena, memmi@unisi.it

Sandra Passchier
Montclair State University, passchiers@mail.montclair.edu

Published in *International Journal of Earth Sciences* (*Geologische Rundschau*), April 2015,
Volume 104, Issue 3, pp 853-872; doi: 10.1007/s00531-014-1117-3

Submitted January 30, 2014; accepted November 24, 2014; published online December 9, 2014.

ORIGINAL PAPER

Early Miocene Antarctic glacial history: New insights from heavy mineral analysis from ANDRILL AND–2A drill core sediments

Francesco Iacoviello, Giovanna Giorgetti, Isabella Turbanti Memmi, and Sandra Passchier

F. Iacoviello (*corresponding*): Instituto Oceanográfico da Universidade de São Paulo, Praça do Oceanográfico, 191, São Paulo, SP 05508–120, Brazil; *Current address:* Department of Chemical Engineering, University College London; email iacoviello.francesco@gmail.com

G. Giorgetti & I. Turbanti Memmi: Dipartimento di Scienze Fisiche, della Terra e dell'Ambiente, Università di Siena, Via Laterina 8, 53100 Siena, Italy

S. Passchier: Department of Earth and Environmental Studies, Montclair State University, Montclair, NJ 07043, USA

Abstract
The present study deals with heavy mineral analysis of late Early Miocene marine sediments recovered in the McMurdo Sound region (Ross Sea, Antarctica) during the ANDRILL—SMS Project in 2007. The main objective is to investigate how heavy mineral assemblages reflect different source rocks and hence different provenance areas. These data contribute to a better understanding of East Antarctica ice dynamics in the Ross Sea sector during the Early Miocene (17.6–20.2 Ma), a time of long-term global warming and sea level rise. The AND-2A drill core recovered several stratigraphic intervals that span from Early Miocene to Pleistocene and it collected a variety of terrigenous lithologies. The heavy mineral assemblages of the lower 650-m-thick sedimentary succession were analyzed through SEM observations and SEM–EDS microanalyses on heavy mineral grains. The heavy mineral analysis shows that the sediments are a mix of detritus dominated by McMurdo Volcanic Group sources most likely located in the present-day Mount Morning area (Proto-Mount Morning) with minor contribution from Transantarctic Mountains source rocks located west of the drill site. The heavy mineral assemblages in Interval 1 indicate that between 20.2 and 20.1 Ma, the grounding line of the ice sheet advanced to a position near the present-day Mount Morning volcanic center. During deposition of Interval 2 (20.1–19.3 Ma), the ice sheet most likely experienced a dynamic behavior with interval of ice advance alternating with periods of ice retreat, while Interval 3 (19.3–18.7 Ma) records further retreat to open water conditions. A dynamic behavior is noted in Interval 4 (18.7–17.6 Ma) with a decreasing contribution of materials derived from the basalts of the Mount Morning volcanic center located to the south of the drill site and a consequent increasing contribution of materials derived from the Transantarctic Mountains to the west of the drill site.
Keywords: Antarctica, ANDRILL, Early Miocene, Heavy mineral analysis, Ice sheet, Ross Sea

Introduction

In recent years, our understanding of the Antarctic ice sheet history in southern Victoria Land has been significantly improved through the study of sediments recovered by drill cores offshore (Barrett et al. 2000; Hambrey and Barrett 1993; Fielding and Thomson 1999; Naish et al. 2007; Harwood et al. 2008). In 2007, the ANtarctic geological DRILLing program (ANDRILL) recovered sediments from 1,138.54 m of drill core in the AND-2A drill hole (Southern McMurdo Sound—SMS; Florindo et al. 2008; Figure 1), which includes an exceptionally well-recovered late Early Miocene section dated 20.2–16.7 Ma.

This paper focuses on the Early Miocene heavy mineral assemblages in the ANDRILL AND-2A drill core, which was recovered near the terminus of a present-day glacier discharging through the Transantarctic Mountains. A previous study by Hauptvogel and Passchier (2012) addressed the ice dynamics in McMurdo Sound during the Miocene Climatic Optimum

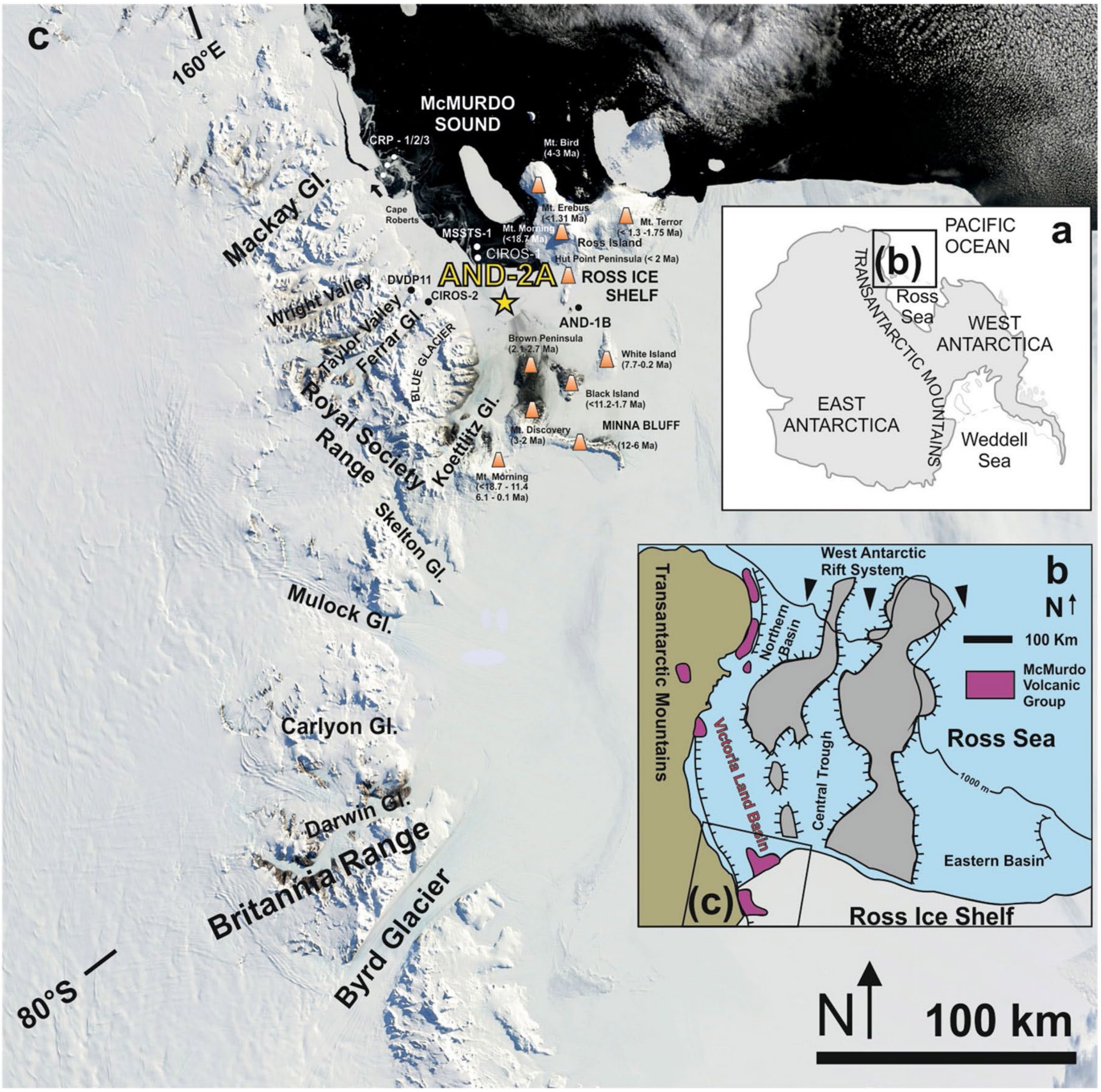

Figure 1. Location of AND-2A drill site in Southern McMurdo Sound. The AND-1B, Cape Roberts Drilling Project (CRP), DVDP11, MSSTS-1, CIROS-1 and CIROS-2 drill sites are also indicated. Ross Island and the Mount Discovery volcanic centers were not present in the late Early to Middle Miocene. Map also shows volcanic centers belonging to the Erebus Volcanic Province with relative time span of activity (Di Vincenzo et al. 2010). *Inset b* has been redrawn and modified after Fielding et al. (2008b).

using the provenance of heavy minerals in the upper 650 m of AND-2A to track areas of maximum glacial erosion under the margin of the East Antarctic Ice Sheet. The late Early Miocene part of the AND-2A record below 650 mbsf is of interest, because it developed during the period of gradual long-term warming and rising sea level leading up to the Miocene Climatic Optimum (Kominz et al. 2008; Cramer et al. 2011; Liebrand et al. 2011).

Because the recovered sediments consist mainly of terrestrial components made available by erosion under the margins of an ice sheet, the heavy mineral assemblages are good indicators of the position of the ice edge in the source areas of the sediments and a valuable tool for reconstructing the glacial history of the Antarctic hinterland and the dynamics of the ice masses (cf. Hauptvogel and Passchier 2012).

The AND-2A drill core recovered a sedimentary sequence with 98 % recovery within an Early Miocene to Quaternary succession punctuated by several disconformities (Harwood et al. 2009). Ages are based on a combination of 40Ar–39Ar geochronology of volcanic material, diatom and foram biostratigraphy, magnetostratigraphy, and Sr-isotope chronology of shell material (Acton et al. 2008, modified after ANDRILL SMS Science Team 2010; Di Vincenzo et al. 2010). This core contains a range of lithologies, including terrigenous clastic diamictites,

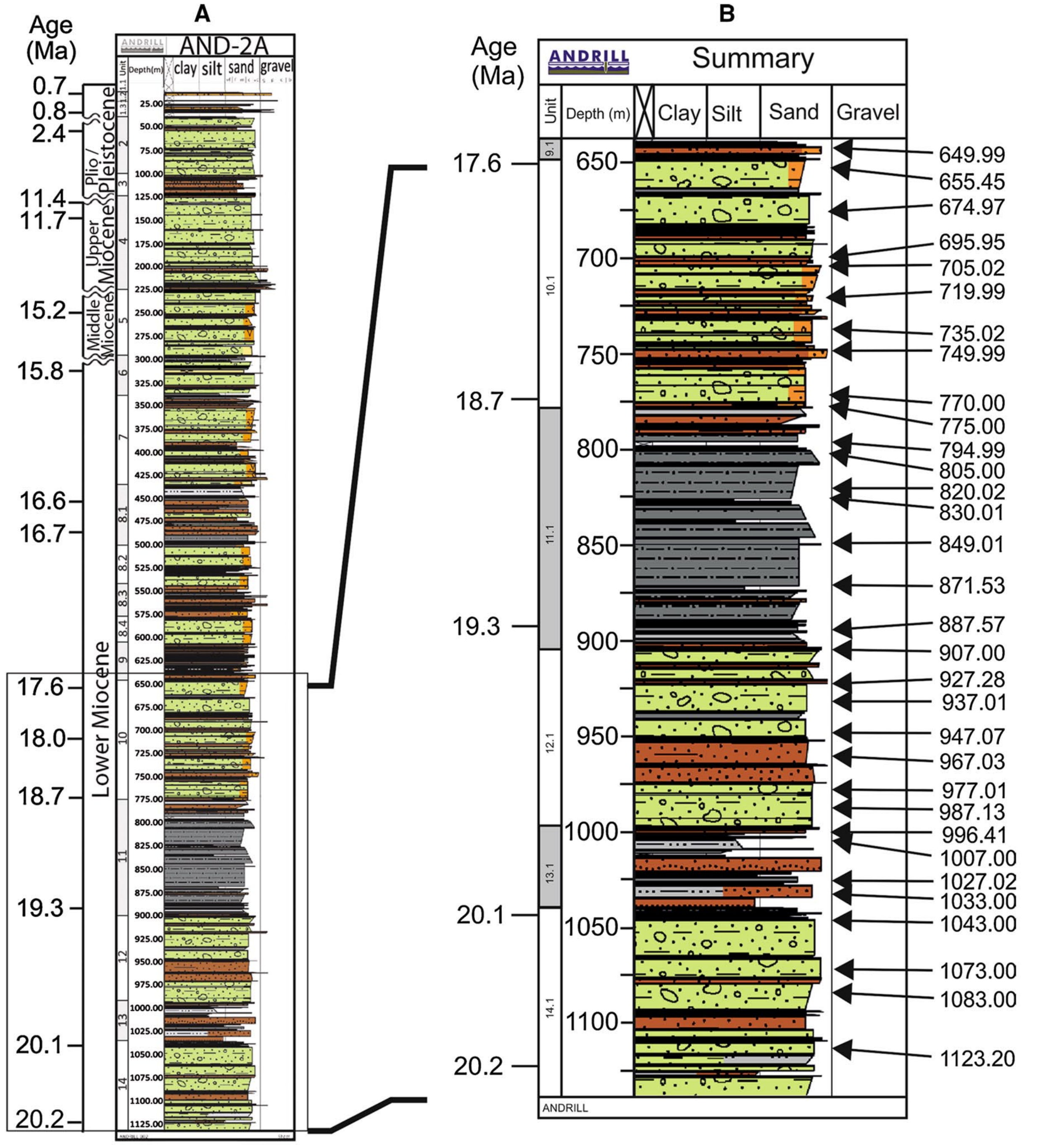

Figure 2. Stratigraphic summary of the AND-2A drill core. Lithologies are plotted against depth. *Green* diamictites, *brown* sandstones, *gray* mudstones, *orange* volcaniclastic sediments. Lithology and chronostratigraphy follow Fielding et al. (2008a), Acton et al. (2008), with modifications reported by ANDRILL SMS Science Team 2010) and Di Vincenzo et al. (2010). **a.** Entire drill core view. **b.** Distribution of investigated heavy mineral samples in the AND-2A core, from 650 to 1,123 mbsf.

conglomerate and breccias, volcanic lava breccias, diatomites, sandstones and mudrocks, pyroclastic and reworked volcanic sedimentary rocks (Fielding et al. 2008a; Figure 2a).

Three fundamentally different paleoclimate regimes are interpreted by Passchier et al. (2011) based on facies associations in AND-2A, and in the Early Miocene section below 650 mbsf these facies associations have the following distribution:

1. A diamictite-dominated facies association that represents glacially dominated depositional environments, including subglacial environments, with only brief intervals where ice-free coasts existed, and time periods when the ice sheet was periodically more expansive than the modern ice sheet. This facies association is present between 648–786, 905–937 and 1,040– 1,138 mbsf.

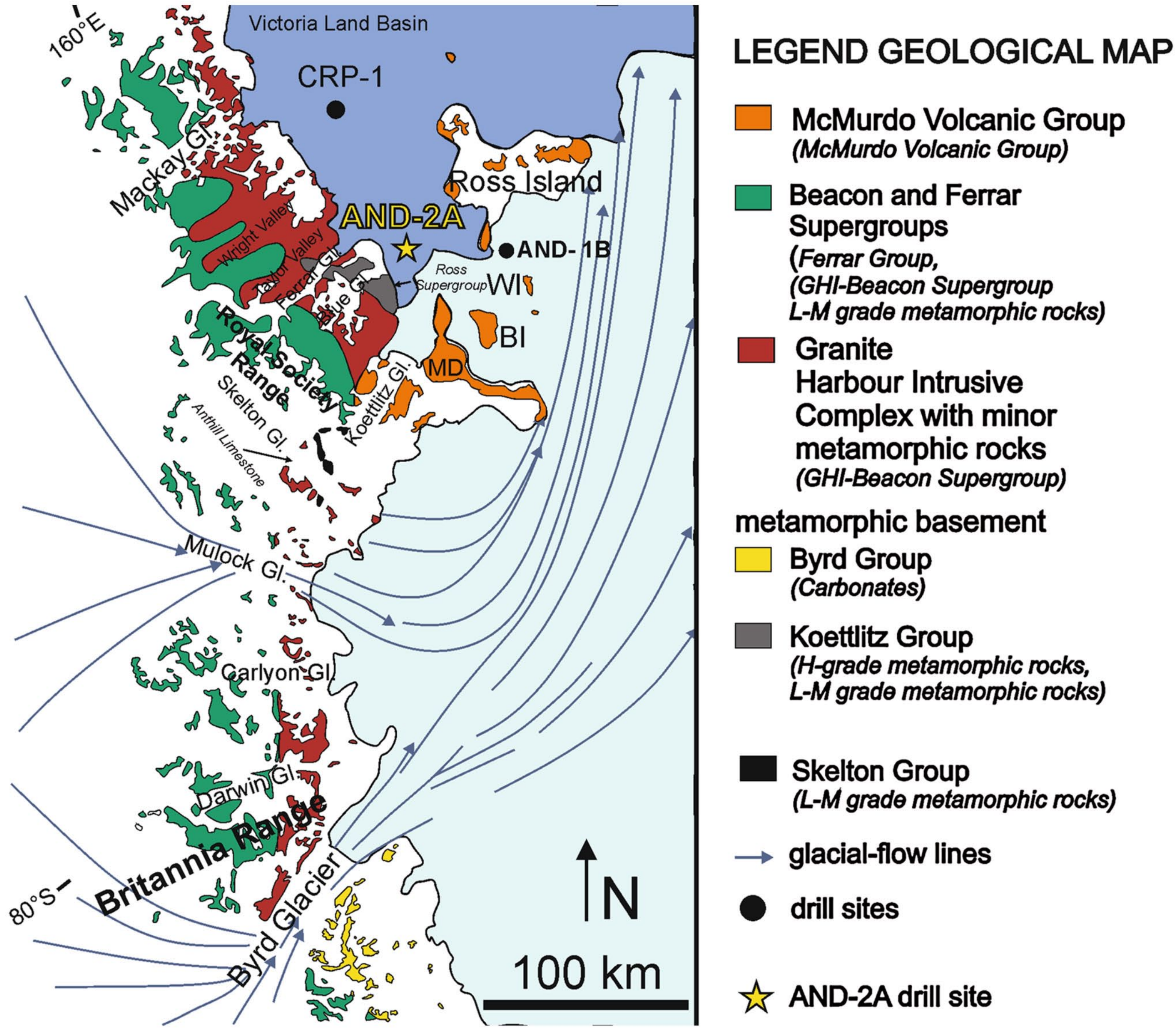

Figure 3. Geological sketch map of the southern Victoria Land (after Gunn and Warren 1962; Warren 1969; Talarico and Sandroni 2011) overlapped on a present-day satellite image (LIMA image provided at the http://lima.usgs.gov/ web site). The present-day glacial-flow directions of major glaciers are also shown (after Fahnestock et al. 2000). *BI* Black Island, *MD* Mount Discovery, *WI* White Island. The location of ANDRILL McMurdo Sound Project (AND-2A) drill site, Cape Roberts Project 1 (CRP-1) drill site and ANDRILL McMurdo Ice Shelf Project (AND-1B) drill site is also shown in the map. In the legend are indicated in *brackets* the possible source rocks discussed in the text.

2. A stratified diamictite and mudstone facies association that includes facies characteristic of open marine to iceberg-influenced depositional environments, and it is more compatible with a very dynamic ice sheet, with a grounding line south of the modern position. This facies association is present between 937– 1,040 mbsf.
3. A mudstone-dominated facies association that generally lacks diamictites, and it was produced in hemipelagic depositional environment influenced by ice. This facies association occurs in the interval 786–905 mbsf.

Geological setting

The AND-2A drill site is located in the McMurdo Sound, a small marginal basin in the southwestern part of the Ross Sea (77°45.488′S; 165°16.613′E; Figures 1, 3). The Ross Sea area is especially suitable for studying the Cenozoic glacial history, because large parts of both the present-day West Antarctic ice sheet and the East Antarctic ice sheet discharge into this embayment. The East Antarctic ice sheet drains directly into the Ross Sea by a number of glaciers breaching the Transantarctic Mountains and indirectly by glaciers feeding the Ross Ice Shelf. Two-thirds of the present ice frontage of the Ross Ice Shelf, however, is derived from large ice streams discharging from the West Antarctic ice sheet (Hambrey and Barrett 1993). Thus, the Ross Sea and McMurdo Sound are situated in a strategic position to document the influence of these ice masses through time. The Victoria Land Basin, located to the northwest of the AND-2A drill site (Figures 1, 3) contains ca.14-km-thick sequence of Mesozoic–Cenozoic strata with dominant sediment supply being from the Transantarctic Mountains, followed volumetrically by volcanic detritus from the Erebus Volcanic Province (EVP; Kyle 1990; Kyle et al. 1992; Cooper et al. 2007; Martin et al. 2010; Nyland et al. 2013). The Cenozoic volcanic rocks of the Transantarctic Mountains form the *McMurdo Volcanic Group* which is subdivided on the basis of geographic location into four provinces (LeMasurier and Thomson 1990): (1) Hallett volcanic province, (2) Melbourne volcanic province, (3) Erebus volcanic province, and (4) Southern most volcanic province.

The EVP, which consists of several large shield and stratovolcanoes surrounding and within the Victoria Land Basin (Figures 1, 3), has provided a steady supply of volcanic detritus resulting in enhanced sedimentation rates since ~20 Ma (Fielding et al. 2008a; Di Vincenzo et al. 2010). The Transantarctic Mountains are composed of both metamorphic and granitic detritus, sedimentary rocks of the Beacon Supergroup as well as dolerite of the Ferrar Group. The western Ross Embayment is composed of alkaline volcanic rocks of McMurdo Volcanic Group (MVG) (Figure 3).

The AND-2A drill site is located at the intersection between various components of the West Antarctic Rift System, including the Victoria Land Basin (VLB, a structural half-graben, approximately 350 km long), the Transantarctic Mountains (TAM, a 4-km high mountain range) and eruptive centers of the Cenozoic McMurdo Volcanic Group (Barrett 1979; Wilson 1999; Figure 3). Furthermore, the region is influenced by four significant elements of the Antarctic cryospheric system: the East Antarctic Ice Sheet (EAIS), Ross Ice Shelf (RIS), West Antarctic Ice Sheet (WAIS), and Ross Embayment sea-ice.

The southern McMurdo Sound is bounded to the west by a sector of the TAM, largely uplifted from ca. 55 Ma as a consequence of the evolution of the West Antarctic Rift System (Fitzgerald 1992, 2002). The southern and eastern shores are characterized by the presence of extensive volcanic edifices, belonging to the Cenozoic alkaline McMurdo Volcanic Group—Erebus Volcanic Province (Gunn and Warren 1962; Kyle 1990; Figure 3).

The basement rocks of the TAM mainly consist of late Proterozoic–Cambrian amphibolite facies metamorphic rocks, which were intruded by the Cambrian–Ordovician granitoids of the Granite Harbour Intrusive Complex (Gunn and Warren 1962; Fitzgerald 2002; Goodge 2007; Sandroni and Talarico 2011). In southern Victoria Land (Figures 1, 3), the basement complex is composed of metamorphic rocks of the Koettlitz Group (medium to high metamorphic grade), exposed between the Ferrar and Koettlitz glaciers, and by the Skelton Group (low-grade metasedimentary rocks), mainly limited to the area near the Skelton Glacier (Cook and Craw 2002). The metamorphic groups are intruded by numerous plutons (Cambrian—Early Ordovician Granite Harbour Intrusive Complex; Gunn and Warren 1962), ranging in composition from granites to gabbros. The Kukri Peneplain is the consequence of uplift and erosion of plutons, and it represents the substratum for the deposition of the sedimentary succession of the Devonian to Triassic Beacon Supergroup (McKelvey et al. 1977). During the Jurassic, both crystalline basement and sedimentary cover were intruded by large doleritic sills and dykes of the Ferrar Supergroup, as a consequence of Gondwana break-up (Elliott 1992; Marsh 2004; Bédard et al. 2007; Zavala et al. 2011).

The Erebus Volcanic Province of the McMurdo Volcanic Group represents the youngest rocks outcropping in this region (Kyle 1990). The extensive alkaline volcanic activity occurred in Cenozoic time during two main phases, the first one that spans between 19 to ca. 10 Ma and the more voluminous and extensive period of volcanic activity occurred since 6 Ma. The composition of most of the deposits from the EVP belong to the strongly silica-undersaturated basanite– tephrite–phonolite alkaline association, although older deposits on Mount Morning are silica-saturated to oversaturated and belong to the alkali basalt–trachyte to rhyolite association (Martin et al. 2010). Mount Morning is considered the source of Early to Middle Miocene volcanic material recovered from the Cape Roberts (Barrett 2007), AND-1B (Pompilio et al. 2007; Di Roberto et al. 2013) and AND-2A cores (Panter et al. 2008; Di Vincenzo et al. 2010; Di Roberto et al. 2012; Nyland et al. 2013). However, indirect evidence of an older volcanic activity (Late Oligocene) has been found within sediments of the Ross Sea Victoria Land Basin recovered by the CIROS-1 and the CRP-2A drill cores (Smellie 2000; Sandroni and Talarico 2004; Zattin et al. 2012).

Subsidence associated with rifting and volcanic loading has generated Early Cenozoic to Quaternary stratigraphic accommodation space adjacent to the rising TAM (Fielding et al. 2006). The combination of a high sediment supply from the TAM and the accommodation space provided by rifting and subsidence of the VLB has protected the sediments from the erosive effects of glaciers that often removed other Antarctic ice-proximal records. Upper Eocene sediments are the oldest post-Paleozoic sediments recovered to date by stratigraphic drilling along the western margin of the basin as documented by the CIROS-1 drill core (e.g., Wilson et al. 1998). These Eocene

Table 1. Source of heavy minerals in the lower part of AND-2A drill core

Source rock	Heavy mineral assemblages
McMurdo Volcanic group	Titanaugite, high-Ca augite (clinopyroxene-2), aenigmatite
	Kaersutite, spinels, ilmenite, apatite angular
Ferrar group	Low-Ca augite (clinopyroxene-1), orthopyroxene
High-grade metamorphic	Andalusite, kyanite, sillimanite
Carbonates	Calcite, dolomite
Granite Harbour Intrusive—Beacon Supergroup	Apatite rounded, zircon, sphene, tourmaline, epidote, rutile, hedenbergite
Low- to medium-grade metamorphic	Hornblende, garnet, biotite, orthoamphibole

strata unconformably overlie Devonian sediments of the Taylor Group (Davey et al. 2001; Paulsen et al. 2011).

The gravel clast components of sediments recovered in AND-2A are derived from the segment of the TAM located between outlet glaciers of the EAIS (Ferrar Glacier–Mulock Glacier regions) and from several volcanic centers of the Late Neogene Erebus Volcanic Province, which are distributed around the southern McMurdo Sound (Panter et al. 2008; Sandroni and Talarico 2011). The Byrd Group farther south constitutes a source of carbonate rocks (Stump et al. 2004, 2006), and detrital carbonate is found in extremely large abundances in Pleistocene tills of the lower Byrd Glacier (Licht et al. 2005).

Provenance analysis

Iacoviello et al. (2012) previously carried out a detailed petrographic survey on clay minerals in the AND-2A drill and found that in the lower 650 mbsf the interpretation of the clay provenance was hindered by authigenic growth of smectites. The occurrence of authigenic smectites and other minerals (calcite and framboidal pyrite) in these intervals indicated that the high smectite contents were probably caused by diagenetic processes (Iacoviello et al. 2012). The low abundance of detrital clay minerals, which reflect the nature of the source areas, made it necessary to examine detrital minerals in the coarse fraction as well. For this reason, heavy minerals were extracted from the sand fraction of samples below 650 mbsf and assemblages were analyzed in order to better reconstruct sediment provenance.

Heavy mineral analysis is among the most common method employed to characterize the composition of coarse marine sediments and to acquire information on sediment provenance (Morton 1985; Dill 1998; Rimington et al. 2000; Wong 2002; Okay and Ergün 2005). Previous studies of heavy minerals carried out on Antarctic marine sediments have shown how heavy mineral assemblages can be used to identify different sediment source areas and to obtain information about the ice sheet dynamics (Diekmann and Kuhn 1999; Ehrmann and Polozek 1999; Polozek 2000; Neumann 2001; Giorgetti et al. 2009; Hauptvogel and Passchier 2012).

Heavy mineral assemblages in sediments can be related to their source rocks through both their chemical composition via SEM–EDS and optical characteristics (e.g., Ehrmann and Polozek 1999; Passchier 2001; Damiani and Giorgetti 2008; Hauptvogel and Passchier 2012). Furthermore, changes in heavy mineral assemblages can be used to identify changes in source regions (e.g., Gwyn and Dreimanis 1979; Diekmann and Kuhn 1999; Polozek and Ehrmann 1998; Passchier 2007; Damiani and Giorgetti 2008; Giorgetti et al. 2009; Hauptvogel and Passchier 2012).

In order to establish the main source rocks of heavy minerals found in our AND-2A samples, we have based our provenance reconstructions on sediment sources already identified by Hauptvogel and Passchier (2012), who analyzed the upper 650 m of the same drill core. In order to reconstruct the paleo flow patterns of the ice from the heavy mineral distributions, these authors incorporated information from facies analysis (Passchier et al. 2011). The presence of shear fabrics and diamictite-dominated facies associations in certain intervals was interpreted to reflect times when the grounding line of the Antarctic Ice Sheet was proximal to the location of the AND-2A drill core during glacial maxima (Passchier et al. 2011). The presence of stratified diamictites and mudstone-dominated facies associations was considered to indicate the existence of open-marine conditions significantly downstream of the ice sheet grounding line during both peak glacial and interglacial conditions (Passchier et al. 2011). They then identified six main source rocks on the basis of their heavy mineral assemblages, which we utilize here in the present study to track the relative contribution of subglacial erosion (Table 1; Figure 3): (1) McMurdo Volcanic Group rocks, located directly to the south and east of the drill site, (2) the Ferrar Group, (3) high-grade metamorphic basement rocks, and (4) carbonates, all located in the upland regions of the Transantarctic Mountains, (5) Granite Harbour Intrusives–Beacon Supergroup, and (6) low- to medium-grade metamorphic rocks exposed along the coast of the Transantarctic Mountains.

It is further noted that the sand mineralogy of primary glacial sediment generally records the composition of rocks eroded up to only several hundreds of kilometers upstream from the glacial terminus (Gwyn and Dreimanis 1979), due to processes of glacial comminution which tend to reduce the size of primary minerals to silt-sized grains (Dreimanis and Vagners 1972; Passchier 2007). Only stable minerals, such as zircon, potentially survive long-term glacial transport in the sand fraction. Lastly, the assemblages are expected to record patterns of glacial erosion during glacial maxima of orbital-scale oscillations of the ice margin, because coarser sand-rich facies are sampled for heavy mineral analysis.

Materials and methods

A total of 32 heavy mineral samples were analyzed starting from 650.00 to 1,123.20 mbsf. Samples were selected in order to achieve coherent sample spacing (~15 m) along the investigated section (Figure 2b). Heavy mineral separation from the sand fraction was carried out in a centrifuge operated at 2,900 RPM for 10 min, using a sodium polytungstate solution with a density of 2.90 g cm^{-3} (Callahan 1987). After centrifugation, the bottom part of plastic funnels containing the heavy mineral fraction was frozen through immersion in liquid nitrogen (N2) so that it did not mix with the light fraction when the funnel was emptied. Afterward, heavy minerals were carefully washed with deionized water and dried on filter papers. Subsequently, heavy minerals from each sample were mounted on a glass slide, carbon coated and viewed using a SEM–EDS (Philips XL30 SEM) equipped with an energy dispersive X-ray detection system (EDAX) at the University of Siena, Italy.

Following Hanan and Totten (1996), grain mineralogies were determined through chemical analyses by EDS and mineral shape, the latter obtained by back scattered electron imaging. Through EDS chemical analysis, it was possible to distinguish between pyroxenes (Fe–Mg pyroxenes, diopsides, titanaugites), amphiboles and oxides. Understanding the chemical composition of pyroxenes and amphiboles is fundamental in order to assign them to different source rocks. All clinopyroxene analyses were plotted on a quadrilateral diagram marked with fields representing the chemical composition of pyroxenes from the Erebus Volcanic Province (after Gamble et al. 1986, dark gray) and the Ferrar Province (after Haban and Elliot 1985, light gray) (Figure 4).

The abundance of each mineral was calculated as a percentage of the total grains counted (n = 200) for each sample. Errors were estimated from repeated measurements (n = 3) on three separates of the same sample and were lower than 6 %. Semi-quantitative chemical analyses for each mineral species were obtained.

Discriminant function analysis (DFA) determines a linear combination of variables (in this study, heavy mineral contents). Variation of one or more of these variables allows the discrimination of predetermined groups following the facies association analysis given by Passchier et al. (2011). The IBM® SPSS 10.0 software package allows the linear combination of variables; these discriminant functions can be used to determine the likelihood of classification of the samples into the predefined groups. Variables that best discriminate between groups have been determined.

Results

Heavy minerals composition

The heavy mineral assemblages of sediments from AND- 2A from greater than 650 mbsf are shown in Figure 4. They are dominated by pyroxenes (augite, titanaugite, aegirine, orthopyroxene and hedenbergite) spinels and ilmenites, whereas amphiboles, carbonates and stable minerals (such as zircon, tourmaline, garnet, rutile and epidote), which are usually common in sediments (Morton and Hallsworth 1999), are present only in minor amounts (Table 2a, b). The chemical compositions of the main silicates are presented in Table 3.

Six types of pyroxenes have been recognized on the basis of their chemical composition (Table 3). Clinopyroxene-1 corresponds to low-Ca augite that falls in the chemical composition field of the Ferrar Province (Figure 4). Low-Ca augites (Table 3; Figure 4) typically show rounded/ sub-rounded shapes and clearly visible cleavage planes (Figure 5a). Clinopyroxene-2 and titanaugite (Table 3; Figure 4) show very similar composition

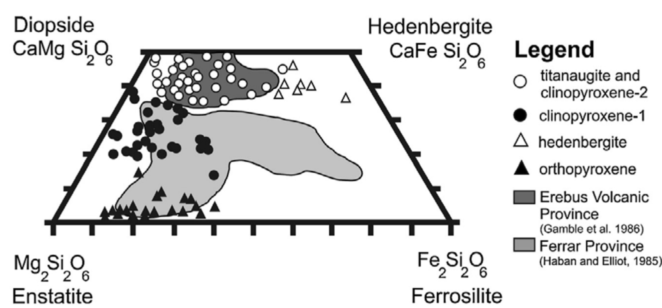

Figure 4. Chemical compositions of pyroxenes from the AND-2A drill core samples. Fields representing chemical composition of pyroxenes from the Erebus Volcanic Province (after Gamble et al. 1986, *dark gray*) and from the Ferrar Province (after Haban and Elliot 1985, *light gray*). *White circles* titanaugite from the MGV and clinopyroxene- 2, *Black circles* clinopyroxene-1 from the Ferrar Group; *White triangles* hedenbergite from the Granite Harbor Intrusive Complex, *Black triangles* orthopyroxene from the Ferrar Group.

Table 2. Percentage counts of heavy minerals for the (a) uppermost, (b) lowermost 16 samples below 650 mbsf of AND-2A drill core

Depth (mbsf)	Sample															
	649.99	655.45	674.97	695.95	705.02	719.99	735.02	749.99	770.00	775.00	794.99	805.00	820.02	830.01	849.01	871.53
(a)																
MVG clinopyroxene	11	9	22	52	45	39	52	54	27	28	30	26	40	41	53	34
Kaersutite	0	0	0	0	4	0	0	0	1	5	0	0	0	5	0	0
Spinels	4	0	4	0	5	17	6	7	2	25	13	16	20	22	8	15
Ilmenite	2	4	0	6	1	8	4	7	7	6	16	18	8	4	8	10
Apatite-1	0	0	0	1	0	0	0	0	0	0	7	3	0	0	0	0
Aegirine	1	0	0	0	1	0	1	0	0	4	5	10	10	1	0	8
Aenigmatite	0	0	0	0	0	0	0	3	0	0	0	0	0	1	0	0
Hornblende	0	0	0	0	1	2	0	0	1	0	0	8	2	1	3	2
Augite	4	1	24	7	4	13	2	1	21	15	13	15	5	5	3	5
Orthopyroxene	37	36	27	31	20	12	18	10	26	4	0	0	5	5	5	3
Garnet	8	4	1	0	2	1	6	0	9	1	2	0	0	1	0	0
Biotite	5	15	1	1	0	1	4	1	3	5	2	0	3	0	3	10
Al–silicate	0	0	0	0	0	0	1	0	1	0	0	0	0	0	0	0
Apatite-2	2	0	1	0	0	0	1	0	0	0	7	0	2	0	0	0
Zircon	1	0	0	0	2	1	1	0	0	0	0	2	0	0	0	0
Rutile	0	0	0	0	1	1	2	0	0	0	0	0	0	0	0	0
Carbonate	0	25	9	2	9	1	1	12	0	0	5	0	0	0	8	5
Sphene	3	3	6	0	1	0	1	0	0	0	0	2	0	4	0	3
Orthoamphibole	16	0	1	0	4	3	0	3	2	2	0	0	3	0	5	3
Tourmaline	1	0	0	0	0	0	0	0	0	0	0	0	0	0	0	0
Epidote	6	1	4	0	1	1	0	0	0	0	0	0	0	0	0	0
Hedenbergite	0	0	0	0	1	0	1	0	0	3	0	0	2	10	8	0

Depth (mbsf)	Sample															
	887.57	907.00	927.28	937.01	947.07	967.03	977.01	987.13	996.41	1,007.00	1027.02	1,033.00	1,043.00	1,073.00	1,083.00	1,123.20
(b)																
MVG Clinopyroxene	20	8	5	9	61	31	20	44	24	5	0	14	87	53	61	42
Kaersutite	0	4	0	0	0	8	1	0	12	0	0	0	0	0	0	0
Spinels	22	20	8	9	11	1	4	13	3	9	0	0	2	9	5	0
Ilmenite	21	12	5	6	3	7	14	3	12	6	0	4	0	25	9	3
Apatite-1	7	0	3	1	0	0	1	4	3	0	0	0	0	2	4	0
Aegirine	6	0	0	4	0	0	1	4	0	0	0	0	2	2	5	0
Aenigmatite	0	0	0	0	0	0	0	0	1	0	0	0	0	0	0	0
Hornblende	0	0	0	0	0	10	9	8	6	0	0	0	4	0	0	15

Table 2. (*continued*)

Depth (mbsf)	Sample															
	887.57	907.00	927.28	937.01	947.07	967.03	977.01	987.13	996.41	1,007.00	1027.02	1,033.00	1,043.00	1,073.00	1,083.00	1,123.20
Augite	6	0	17	12	3	7	10	9	4	5	0	0	2	5	10	7
Orthopyroxene	4	0	8	9	0	0	1	0	1	12	0	0	4	0	0	0
Garnet	6	4	14	12	3	17	4	8	11	26	57	3	0	2	3	8
Biotite	4	23	4	11	0	6	2	0	1	11	4	52	0	2	0	0
Al–silicate	0	0	0	0	0	0	0	0	0	4	0	0	0	0	0	2
Apatite-2	3	4	4	6	0	2	5	1	5	7	0	3	0	2	0	7
Zircon	0	3	1	2	0	1	2	2	0	0	0	1	0	0	0	0
Rutile	0	1	0	0	0	0	1	2	0	0	0	1	0	0	0	0
Carbonate	0	0	26	16	17	0	4	0	8	10	0	0	0	0	0	2
Sphene	1	3	3	2	3	0	6	0	0	5	0	4	0	0	4	3
Orthoamphibole	0	16	0	0	0	8	12	2	8	0	25	16	0	0	0	8
Tourmaline	1	1	0	0	0	3	0	0	3	0	14	0	0	0	0	0
Epidote	0	1	3	0	0	0	5	2	0	0	0	0	0	0	0	3
Hedenbergite	0	0	0	0	0	0	0	0	0	0	0	0	0	0	1	0

except for the Ti and Al contents and fall in the McMurdo Volcanic Group field (Figure 4). Clinopyroxene-2 has the chemical composition of diopside. Titanaugite and clinopyroxene-2 are the most abundant phases and occur as very irregular crystals with visible hacksaw terminations (Figure 5b, c, respectively). Due to their chemical and morphological similarities, these two types of pyroxenes were classified into the same group called *MVG (McMurdo Volcanic Group) clinopyroxene*. Hedenbergites (Table 3; Figure 4) typically display euhedral crystals (Figure 5d). Alkaline pyroxenes such as aegirine have also been recognized (Table 3), and they generally show cleavage (Figure 5e). The orthopyroxene group (Table 3; Figure 4) comprises Mg-rich pyroxene, including pigeonites. Orthopyroxenes usually show an elongated shape with visible cleavage (Figure 5f).

Apatite grains occur with two kinds of morphologies: apatite-1 (angular apatite) shows euhedral crystal with visible crystal faces (Figure 5g), whereas apatite-2 (rounded apatite) shows sub-rounded-shaped crystals with fracture plates (Figure 5h). Spinel and ilmenite are quite common phases and occur as sub-euhedral crystals (Figure 5i). Garnet grains have a chemical composition varying from almandine to spessartine and grossular end members (Table 3). They usually occur with sub-rounded shapes and smooth edges (Figure 5j). An aluminosilicate (Al_2SiO_5) is also recognized. Three types of amphiboles are distinguished: hornblende, kaersutite and orthoamphibole gedrite (Table 3; Figure 5k, l). Carbonate grains, both calcite and dolomite, have been merged into the same group called *carbonate*.

Heavy mineral down-core distribution

Figure 6 shows the down-core variation in abundances of the main heavy mineral phases in the Early Miocene section below 650 mbsf. MVG clinopyroxenes show the highest percent by volume and the largest variation in abundance of all minerals. MVG clinopyroxenes shows oscillations between 887 and 1,043 mbsf and displays the highest percentages below 1,043 mbsf. Augite and orthopyroxene occur throughout the core and are particularly abundant in the upper part of the investigated section between 650 and 770 mbsf as well as between 890 and 1,043 mbsf. The percentages of MVG clinopyroxene and Ferrar Group augite show an opposite trend, as well as MVG clinopyroxene and Ferrar Group orthopyroxenes. On the contrary, abundances of augite and orthopyroxene co-vary. Kaersutite and aenigmatite occur in very low amount, and it is not possible to recognize a down-core trend.

Spinel, ilmenite, apatite-1 (angular) and aegirine covary and they are particularly abundant between 770 and 890 mbsf, with higher percentage oscillation between 890 and 1,043 mbsf. Spinel and ilmenite display a very similar trend.

Table 3. Average chemical compositions of abundant heavy minerals as determined by SEM–EDS analysis

Mineral	Data type	Na_2O	MgO	Al_2O_3	SiO_2	K_2O	CaO	TiO_2	Cr_2O_3	MnO	FeO	Na	Mg	Al	Si	K	Ca	Ti	Cr	Mn	Fe
Clinopyroxene-1	Average	0.98	17.76	3.04	53.29	0.23	14.98	0.32	0.24	0.34	8.84	0.1	1.0	0.1	2.0	0.0	0.6	0.0	0.0	0.0	0.3
	STDEV	0.36	2.97	1.90	1.74	0.31	4.22	0.13	0.17	0.21	5.28	0.0	0.1	0.1	0.0	0.0	0.2	0.0	0.0	0.0	0.2
Clinopyroxene-2	Average	0.86	13.74	1.64	52.32	0.09	23.16	0.23	0.39	0.50	7.10	0.1	0.8	0.1	2.0	0.0	0.9	0.0	0.0	0.0	0.2
	STDEV	0.30	2.80	0.77	1.70	0.08	1.53	0.19	0.20	0.18	3.04	0.0	0.1	0.0	0.0	0.0	0.1	0.0	0.0	0.0	0.1
Titanaugite	Average	1.05	13.94	6.33	47.79	0.05	20.48	2.27	0.20	0.23	7.66	0.1	0.8	0.3	1.8	0.0	0.8	0.1	0.0	0.0	0.2
	STDEV	0.30	1.28	1.23	1.56	0.05	1.60	0.74	0.12	0.14	1.13	0.0	0.1	0.1	0.1	0.0	0.1	0.0	0.0	0.0	0.0
Orthopyroxene	Average	1.21	23.83	2.49	55.18	0.21	2.48	0.27	0.22	0.48	13.65	0.1	1.3	0.1	2.0	0.0	0.1	0.0	0.0	0.0	0.4
	STDEV	0.53	4.18	1.04	2.24	0.12	1.01	0.09	0.14	0.10	4.40	0.0	0.2	0.0	0.1	0.0	0.0	0.0	0.0	0.0	0.1
Aegirine	Average	14.85	1.50	2.08	55.94	0.15	0.75	1.84	0.11	1.06	21.71	1.1	0.1	0.1	2.2	0.0	0.0	0.1	0.0	0.0	0.7
	STDEV	1.38	0.62	0.85	1.79	0.12	0.69	0.90	0.04	0.53	1.56	0.1	0.0	0.0	0.0	0.0	0.0	0.0	0.0	0.0	0.1
Hedenbergite	Average	1.60	3.06	1.13	47.52	0.12	18.94	0.61	0.16	1.48	25.39	0.1	0.2	0.1	1.9	0.0	0.8	0.0	0.0	0.1	0.9
	STDEV	0.53	1.56	0.16	2.50	0.04	1.77	0.16	0.11	0.20	3.87	0.0	0.1	0.0	0.1	0.0	0.1	0.0	0.0	0.0	0.2
Hornblende	Average	1.67	12.40	12.27	48.50	0.74	11.74	1.04	0.24	0.55	10.84	0.5	2.6	2.0	6.8	0.1	1.8	0.1	0.0	0.1	1.3
	STDEV	0.12	0.91	2.10	1.29	0.35	3.46	0.74	0.21	0.04	4.13	0.0	0.2	0.3	0.1	0.1	0.5	0.1	0.0	0.0	0.5
Kaersutite	Average	2.15	9.16	13.18	42.52	2.13	8.82	3.23	0.10	0.46	18.24	0.6	2.0	2.3	6.3	0.4	1.4	0.4	0.0	0.1	2.3
	STDEV	0.78	2.27	2.49	4.26	1.49	4.08	1.21	0.09	0.21	5.26	0.2	0.5	0.4	0.5	0.3	0.6	0.1	0.0	0.0	0.7
Garnet	Average	0.69	1.02	19.34	40.38	0.02	32.47	0.85	0.29	0.34	4.63	0.1	0.1	1.7	3.1	0.0	2.6	0.1	0.0	0.0	0.3
	STDEV	0.45	0.61	3.05	1.39	0.03	0.42	0.91	0.08	0.02	2.14	0.1	0.1	0.2	0.0	0.0	0.1	0.1	0.0	0.0	0.1
Garnet	Average	0.79	8.38	22.62	41.54	0.07	1.48	0.14	0.19	0.86	23.96	0.1	0.9	2.0	3.1	0.0	0.1	0.0	0.0	0.1	1.5
	STDEV	0.78	2.86	0.50	0.92	0.04	0.71	0.08	0.08	0.46	3.93	0.1	0.3	0.0	0.0	0.0	0.1	0.0	0.0	0.0	0.3
Garnet	Average	0.55	4.55	21.76	39.58	0.10	1.05	0.17	0.26	17.47	14.55	0.1	0.5	2.0	3.1	0.0	0.1	0.0	0.0	1.2	1.0
	STDEV	0.45	0.19	0.40	1.41	0.02	0.12	0.02	0.02	3.66	2.55	0.1	0.0	0.0	0.1	0.0	0.0	0.0	0.0	0.3	0.2
Gedrite	Average	0.97	8.65	21.94	40.55	0.17	2.66	0.20	0.21	0.92	23.71	0.3	1.9	3.8	5.9	0.0	0.4	0.0	0.0	0.1	2.9
	STDEV	0.50	2.36	0.92	1.84	0.03	2.91	0.10	0.12	0.34	3.72	0.1	0.5	0.1	0.1	0.0	0.5	0.0	0.0	0.0	0.5

Averages are based on several grains from different locations in the AND-2A drill core. Analyses are given in oxide wt% and recalculated on the basis of negative charges (indicated by the O number).

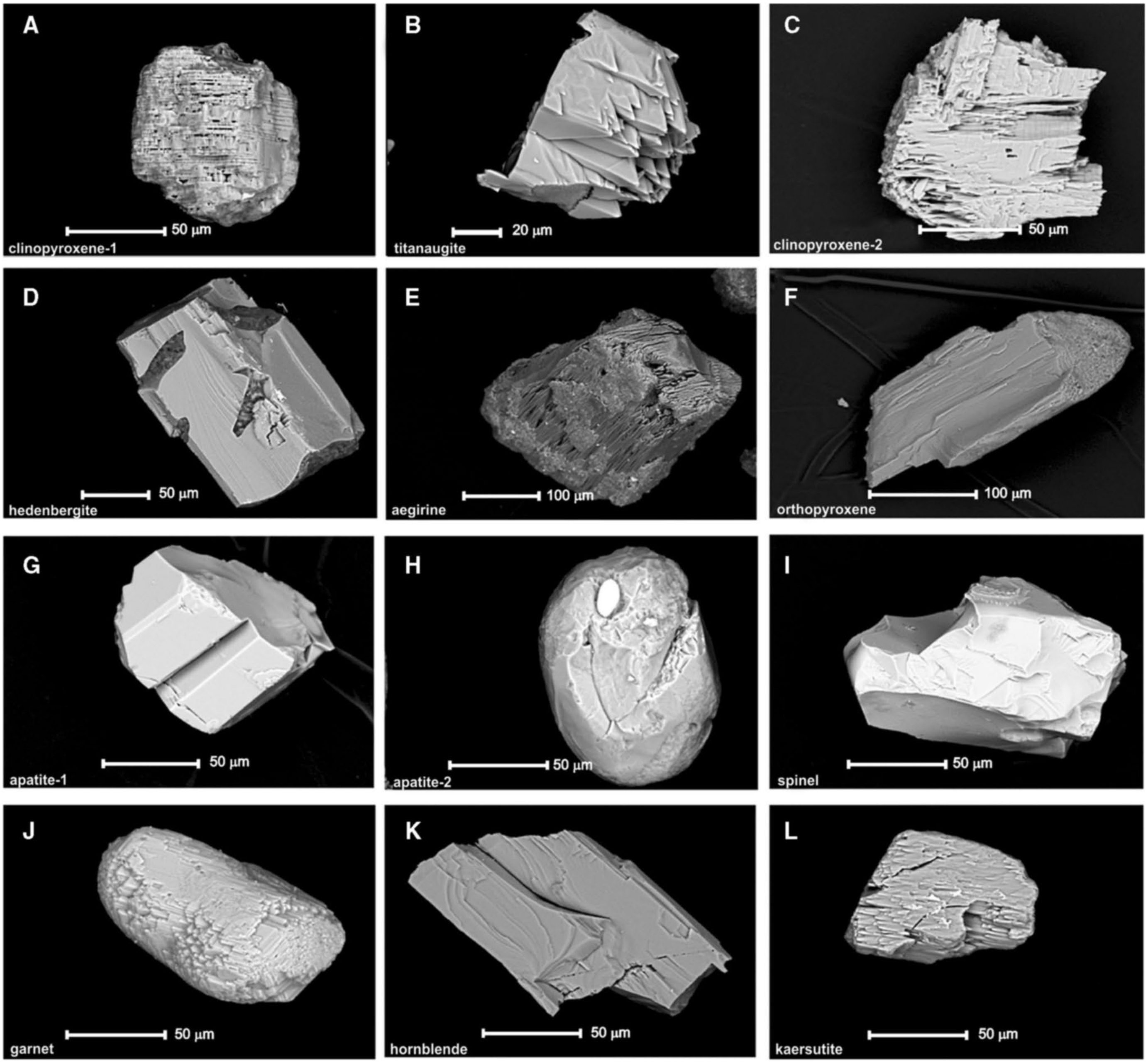

Figure 5. SEM backscattered images of the most common heavy minerals in AND-2A drill core: **a.** clinopyroxene-1 with visible cleavage at 987.13 mbsf; **b.** titanaugite with hacksaw terminations from sample 987.13 mbsf; **c.** clinopyroxene-2 with no visible cleavage and hacksaw termination at 705.02 mbsf; **d.** hedenbergite grain at 820.02 mbsf; **e.** aegirine at 820.02 mbsf; **f.** orthopyroxene grain at 655.45 mbsf; **g.** angular apatite (apatite-1) grain at 996.41 mbsf; **h.** rounded apatite (apatite-2) grain at 987.13 mbsf; **i.** spinel at 820.02 mbsf; **j.** sub-rounded garnet grain at 907.00 mbsf; **k.** hornblende grain at 967.03 mbsf; **l.** kaersutite from sample 967.03 mbsf.

Rutile and zircon display an almost identical down-core trend: in fact, they are present in the interval 700–750 mbsf and show the same peaks of abundance in the interval 890–1,043 mbsf. Sphene and epidote co-vary between 650 and 700 mbsf; they show a high variability, however, in the interval 890–1,043 mbsf and are present again below ~1,075 mbsf.

Garnet is abundant especially in the interval between 890 and 1,043 mbsf and has a maximum at 1,027 mbsf (43 %). Garnet and MVG clinopyroxene show a weak negative correlation. Biotite and orthoamphibole show a similar down-core variation. They occur throughout the core and are particularly abundant in the interval between 890 and 1,043 mbsf. Carbonate is very abundant in the intervals between 650 and 770 mbsf and between 927 and 1,043 mbsf. It displays a negative correlation with MVG clinopyroxenes. Al–silicate has very low percentages. Nonetheless, it is present in the interval between 730 and 770 mbsf, in sample 1,007.00 mbsf, and at 1,123.20 mbsf.

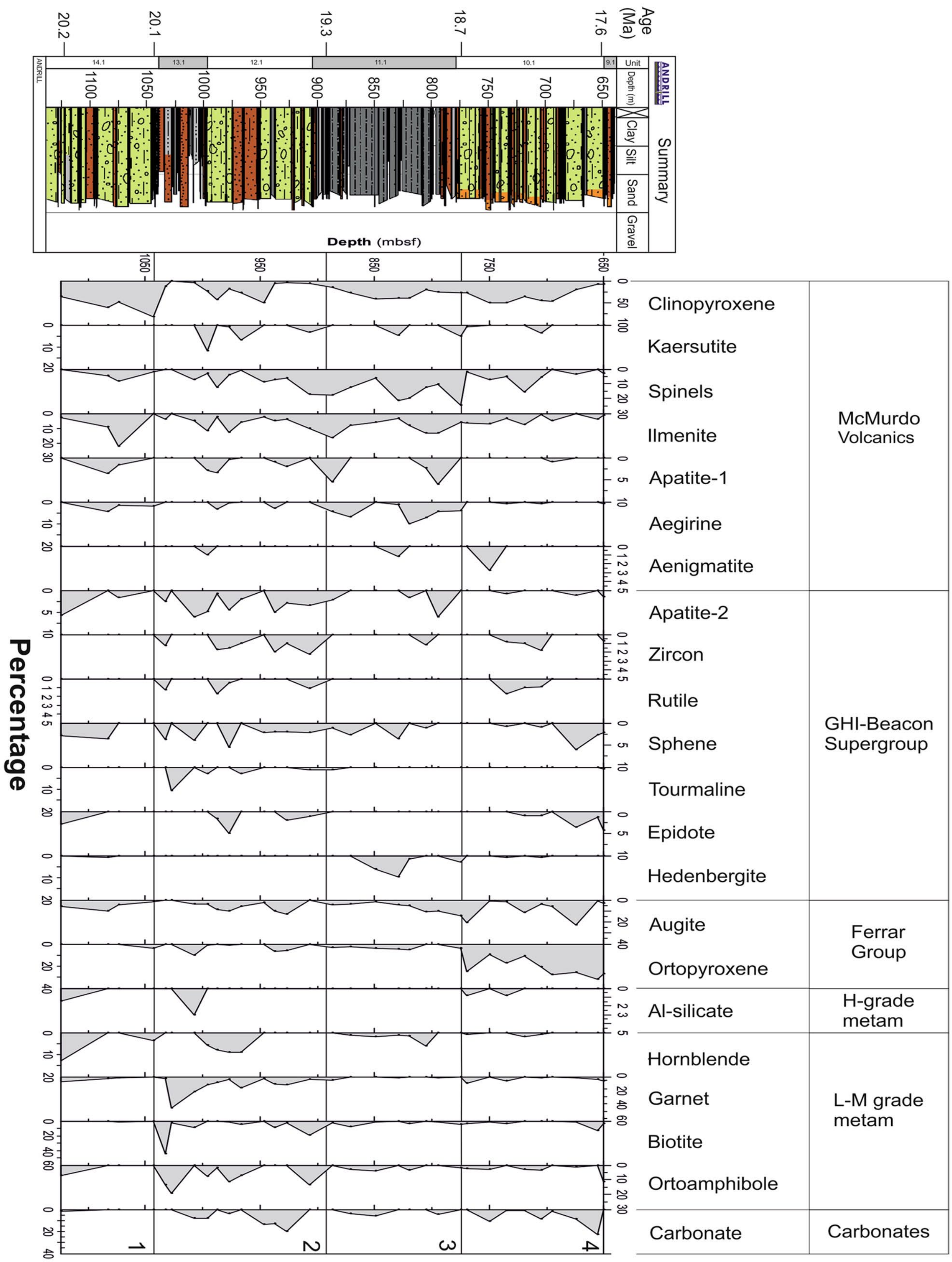

Figure 6. Down-core variation of the main heavy mineral phases present in AND-2A drill core. Groups of sediment provenance are after Hauptvogel and Passchier (2012). GHI indicates Granite Harbour Intrusive.

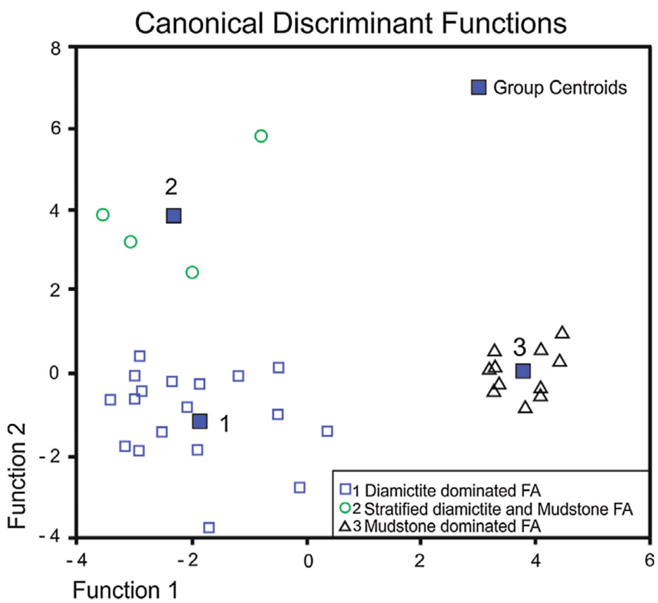

Figure 7. Plot of discriminant scores along Function I versus Function II, to discriminate samples belonging to different sedimentary facies. Group 1 represents diamictites dominated facies association; group 2 refers to stratified diamictites and mudstone facies association; group 3 represents mudstone facies association.

Table 4. Discriminant functions: unstandardized discriminant function coefficients used to calculate discriminant scores for the plot in Figure 7

	Discriminant functions		Structure matrix	
	1	2	1	2
Clinopyroxene	−0.028	0.741	−0.116	0.201
Kaersutite	−0.480	0.535	−0.074	0.023
Spinels	0.011	0.760	0.137	−0.210
Ilmenite	0.002	0.603	0.081	−0.104
Apatite-1	0.154	0.566	0.082	−0.055
Aegirine	0.508	0.576	0.200	−0.025
Aenigmatite	0.251	0.113	−0.020	−0.081
Tourmaline	0.342	1.327	0.065	0.046
Epidote	−1.271	0.318	−0.146	−0.090
Hedenbergite	0.764	0.648	0.117	−0.023
Hornblende	0.121	1.168	−0.073	0.326
Augite	0.005	0.665	−0.045	−0.100
Orthopyroxene	0.064	0.793	−0.111	−0.064
Garnet	−0.030	0.649	0.072	0.033
Biotite	0.021	0.804	0.098	−0.039
Apatite-2	0.496	1.284	0.067	0.072
Carbonate	0.037	0.619	−0.032	−0.159
Sphene	0.348	0.666	0.032	−0.102
Orthoamphibole	0.157	0.523	0.020	0.001
(Constant)	−2.789	−71.531		

Structure matrix: pooled within-groups correlations between discriminating variables and standardized canonical discriminant functions

Heavy mineral facies distribution

The DFA shows that the individual samples can be classified into three predefined groups. The three groups have been defined based on the facies association by Passchier et al. (2011): group 1 refers to diamictite-dominated facies association; group 2 refers to stratified diamictites and mudstone facies association; group 3 comprises sediments that refer to mudstone-dominated facies association deposited in an open-marine environment distal from the grounding line. The results of DFA are illustrated in the territorial map (Figure 7) showing the clustering of samples in the predefined groups, and in Table 4, which reports the coefficients for each variable in the two functions and the structure matrix.

Function 1 correctly discriminates groups 1 and 2 from group 3. The former two groups partially overlap. Aegirine, spinels, hedenbergite and ilmenite have high positive loading on function 1 (Table 4). Hornblende, kaersutite and clinopyroxene have high negative loading on function 1 and high positive loading on function 2 (Table 4). Function 2 discriminates groups 1 and 3 (that show value around zero) from group 2 (which shows values higher than zero). Augite, epidote, orthopyroxenes and carbonates have a negative loading on both function 1 and 2 (Table 4). The diamictite-dominated facies association (group 1) is characterized by a high content of TAM-derived minerals, with prevalence of augites and orthopyroxenes. The stratified diamictites and mudstone facies association (group 2) shows a mixed content of TAM-derived minerals (hornblende) as well as MVG-derived minerals (clinopyroxenes and kaersutite), garnets and orthoamphiboles. Mudstone-dominated facies association (group 3), characteristic of open-marine sediments, is characterized by extremely low TAM mineral content and a relative increase in aegirine, spinel and ilmenite among the MVG phases.

Discussion

Heavy mineral sources

McMurdo Volcanic Group (MVG)

Basic volcanic rocks of the McMurdo Volcanic Group are the source of titanaugite and clinopyroxene-2 (high-Ca augite). The titanaugite compositions clearly fall within the field of MVG clinopyroxene (Figure 4). This type of clinopyroxene represents the most abundant phenocrysts in the McMurdo Volcanic Group lavas (Gamble et al. 1986; George 1989; Kyle 1990). Its euhedral shape in the AND- 2A sediments indicates that it has not experienced the effects of prolonged transport.

Trachytes, basalts and trachyandesites of MVG are the most likely source for kaersutite (Kyle 1990; LeMasurier and Thomson 1990). Moreover, kaersutite is a typical mineral in lava deposits on Minna Bluff (Dunbar et al. 2008; Panter et al. 2011). MVG volcanic rocks are also the source of angular apatite grains. Martin (2009), and Martin et al. (2010) have shown that Mount Morning eruptive center is a potential source of aenigmatite and aegirine.

Ferrar Group

Jurassic basalt and dolerite of the Ferrar Group in the TAM are the most likely source for augites (low-Ca augite) as well as for Mg-rich clinopyroxenes and orthopyroxenes (Haban and Elliot 1985; Armienti et al. 1998). The chemical compositions of augites plot in the field of the Ferrar Supergroup clinopyroxenes (Figure 4; Table 3). The augites with a strong cleavage and sub-rounded shape (Figure 5a) have been named "Ferrar type" in many studies (e.g., Cape Roberts Science Team 1998), and they probably originated from Ferrar Dolerites. Tholeiitic igneous rocks from the Ferrar Group are the most likely source for enstatites (Armienti et al. 1998; Marsh 2004; Bédard et al. 2007; Zavala et al. 2011).

High-grade metamorphic rocks

The H-grade metamorphic rocks of the Koettlitz Group located to the north of the Koettlitz Glacier (Figure 3) could have provided the H-grade metamorphic minerals. Under SEM, it is impossible to discriminate between sillimanite, kyanite and andalusite; hence, we decided to assign them to the same group called *Al-silicates*. Hauptvogel and Passchier (2012) reported that kyanite, not being a common constituent in these rocks, probably requires a contribution of rocks from the Nimrod Group farther south. In addition, Passchier (2001) has found large grains of sillimanite occur in tills sourced from the metaquartzite of the Nimrod Group. Hence, the Al–silicates are not diagnostic for a specific source area.

Carbonates

Anthill Limestone (Gunn and Warren 1962; Skinner 1982), also named Marble Unit by Cook and Craw (2002), which crops out along the margin of the Skelton Glacier (Hauptvogel and Passchier 2012; Figure 3), is the most likely source for calcite and dolomite. The Byrd Group (Figure 3), which crops out farther south, is characterized by the initial deposition of a thick sequence of nearly pure carbonate sediments followed by a thick sequence of clastic sediments (Stump et al. 2004, 2006). Moreover, Pleistocene tills of lower Byrd Glacier contain detrital carbonate in extremely large abundances (Licht et al. 2005). In addition, Passchier (2001) has found limestone-bearing tills in the Queen Maud range in the central Transantarctic Mountains. These tills were probably sourced from the Shackleton Limestone (Goodge et al. 2004). Between the Ferrar and Koettlitz Glaciers, marbles from the Ross Supergroup are also present (Warren 1969; Lopatin 1972).

Granite Harbour Intrusive (GHI)—Beacon Supergroup

Sedimentary rocks of the Beacon Supergroup are the most likely source of the stable minerals (apatite-2, tourmaline, rutile, zircon, sphene and epidote). They usually occur as sub-rounded to rounded grains indicating a possible recycling and transport from rocks of the Beacon Supergroup, which contain both zircon and apatite (Laird and Bradshaw1982; La Prade 1982; Giorgetti et al. 2009). Plutonic rocks and pegmatites of the GHI Complex contain sphene as an accessory constituent (Ghent and Henderson 1968; Smillie 1992). Passchier (2007) suggests the GHI and the Beacon Supergroup as the main sources for detrital apatite. Lower Paleozoic dykes and batholiths of the GHI contain tourmaline in higher abundances (Stump 1995). Hedenbergites have been found in tonalites from the GHI (Sandroni and Talarico 2004).

Low- to medium-grade metamorphic rocks (L–M grade metamorphic rocks)

The Transantarctic Mountains, and in particular, the amphibolites of the Koettlitz Group are the most likely source for Mg-hornblendes: these amphiboles are characteristic minerals of many metamorphic and intermediate magmatic rocks (Polozek 2000). We have also to take into account that hornblendes were described in the granitoids (GHI Complex) of Taylor Valley (Ghent and Henderson 1968; Smillie 1992).

Amphibolites and paragneisses exposed between the Koettlitz and Ferrar Glaciers are the most probable sources for garnets (Figure 3; Lopatin 1972) and occur in significant abundances in the Late Miocene and Pliocene tills of the Ferrar, Taylor and Wright Valleys (Ehrmann and Polozek 1999; Passchier 2001). Some grains have a sub-rounded to rounded shape. Because garnets are resistant to physical weathering during transport, they also could be recycled from sandy sedimentary rocks, such as those of the Beacon Supergroup, where they occur as accessory minerals (Laird and Bradshaw 1982; La Prade

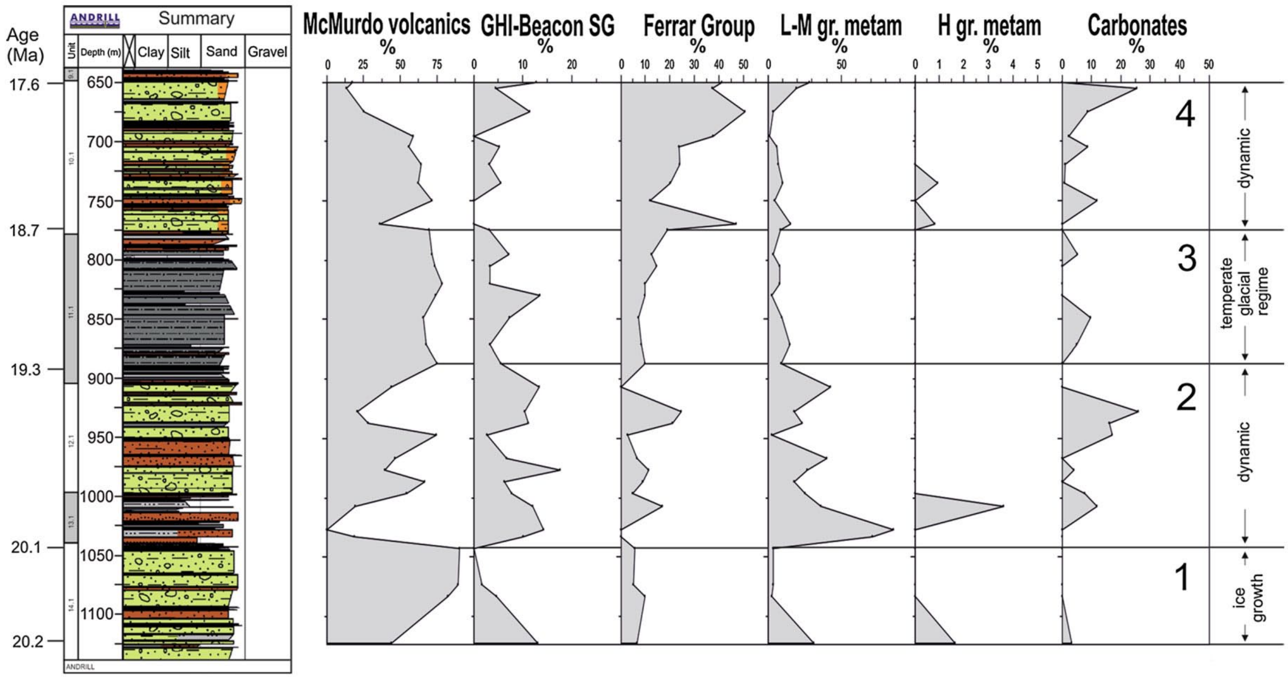

Figure 8. Summary plot of heavy mineral distribution down-core. On the right, the glacial setting configuration inferred from facies distribution in the core (Passchier et al. 2011). The presence of shear fabrics and massive diamictites in core intervals ("ice growth") indicates proximity of the grounding line during glacial maxima, whereas mudstones ("temperate glacial regime") indicate generally open-marine conditions with a grounding line at some distance from the drill site during both glacial maxima and minima (Passchier et al. 2011). Ages (40Ar–39Ar geochronology of volcanic material, Acton et al. 2008; Di Vincenzo et al. 2010) are also reported.

1982). Metasediments and marbles of the Koettlitz Group host pyrope–almandine and grossular garnets. Orthoamphibole gedrite is found in the Cocks unit of the Skelton Group and is associated with garnet and biotite (Cook and Craw 2002). The Skelton Group, exposed along the Skelton Glacier, is considered the source of low-grade metasedimentary clasts (Gunn and Warren 1962; Cook and Craw 2002). In the portions intruded by granitoid plutons, the metasedimentary rocks are in place characterized by a local contact-metamorphic overprint (Gunn and Warren 1962; Skinner 1982), with the development of biotite-spotted and amphibole-bearing varieties.

Heavy mineral distribution

Based on the relative abundance of the heavy mineral assemblages in the core, the lower 650 mbsf is subdivided into four intervals, numbered 1–4 from bottom to top (Figure 8).

The lowermost interval 1 (1,123–1,043 mbsf; 20.2– 20.1 Ma) is characterized by high abundance of heavy minerals derived from the McMurdo Volcanic Group, followed by low- to medium-grade metamorphic rocks and GHI-Beacon Supergroup, as well as Ferrar Group. The heavy mineral assemblage indicates erosion of MVG rocks during ice advance. These results are compatible with a primary (explosive activity) basaltic input from proto-Mount Morning volcanic center to the south of the drill site. Nyland et al. (2013) found out that the majority of AND-2A glass analyzed in the interval 354–765 mbsf is considered to originate from explosive eruptions and was incorporated in basin sediments with minimal reworking. The 345–765 mbsf interval, however, is considerably younger than the interval we are discussing here (1,123–1,043 mbsf) and the facies assemblages and sediment transport paths are very different for these two intervals (Passchier et al. 2011).

Interval 2 (1,043–890 mbsf; 20.1–19.3 Ma) is characterized by large fluctuations in the contribution of sediments eroded from the McMurdo Volcanic Group, which point to a source from the Mount Morning area located to the south. Oscillations of GHI-Beacon Supergroup, Ferrar and L–M grade metamorphic rocks indicate a local source situated in the Transantarctic Mountains. GHI-Beacon Supergroup, Ferrar Group, L–M grade metamorphic rocks and carbonates display a similar trend. The high-grade metamorphic group shows very low counts, but seems to correlate with GHI-Beacon Supergroup, Ferrar Group and Carbonates. Nevertheless, the occurrence of minerals of the high-grade metamorphic group in the lower part of the unit, as suggested by Hauptvogel and Passchier (2012) for the upper 650 mbfs of the AND-2A drill core, could indicate either an erosion of Koettlitz Group, where these minerals are present (Lopatin 1972), or a provenance within the Nimrod Group farther south. Furthermore, for the same interval, Talarico and Sandroni (2011) reported that the metamorphic clast assemblage suggests a provenance in the Carlyon Glacier and

Darwin-Byrd Glacier areas. The clast assemblage is represents rock types with mineral paragenesis like garnet-sillimanite-K-feldspar-biotite, indicating medium/high-grade metamorphic conditions that occur only in the Britannia Range (Figure 3). The compositions of diamictites, interpreted as iceberg-rafted debris (Passchier et al. 2011; Talarico and Sandroni 2011), suggest active calving processes occurred simultaneously along the present-day Blue–Koettlitz glacier coast and from paleoglacier located further south, including the Skelton-Mulock glacier area.

Interval 2 is characterized by a cyclic McMurdo volcanic Group signal, which indicates a repeated contribution from the south, and L–M grade metamorphic, GHI-Beacon Supergroup and Ferrar Group fluctuations, which indicate a heavy mineral assemblage derived from a local source. This pattern can be explained as an advance of the grounding lines of EAIS outlet glaciers to the coast in the southern TAM, where they eroded largely the GHI-Beacon Supergroup rocks, with minor contributions from Ferrar dolerite. Interval 3 (890–770 mbsf; 19.3–18.7 Ma) marks an increase in the McMurdo Volcanic Group signal and a decrease in the Ferrar Group, GHI-Beacon Supergroup, L–M grade metamorphic rock group as well as the carbonate contribution. For this interval, the heavy mineral assemblages indicate erosion of the basalts of the McMurdo Volcanic Group south of the drill site, with limited erosion of low- and high-grade metamorphic rocks of basement. The presence of few grains of aenigmatite (Figure 6) can be considered a fingerprint for heavy minerals of volcanic origin. Clast provenance studies by Talarico and Sandroni (2011) testified a mixed provenance from Royal Society Range area and Skelton-Mulock glacier area (Figures 1, 3), thus helping us to pinpoint a heavy mineral assemblage provenance from an area located south of the drill site.

Although heavy mineral assemblages dominated by McMurdo Volcanic Group contribution in the lower part of interval 3 (770–890 mbsf) indicate a sediment provenance located south of the drill site, the mudstone-dominated facies at 770–890 mbsf (Figure 8) probably indicates an ice sheet in a reduced configuration, with predominantly meltwater plume deposition and minor ice rafting (Passchier et al. 2011). Therefore, an alternative to a glacial transport scenario for this interval must be considered. The probable mechanisms able to transport MVG heavy minerals to the AND-2A drill site in the interval between 770 and 890 mbsf could be the direct fall-out of volcanic material. Support for this hypothesis is found in the paper of Nyland et al. (2013). These authors recognized high abundances (5–70 vol%) of fresh volcanic glass in finer-grained sediments such as siltstone and sandstone between ~230 and 780 mbsf. These observations, however, were made in a considerably younger interval of core with different facies assemblages (Passchier et al. 2011) and hence may or may not be applicable to the Early Miocene section of AND-2A.

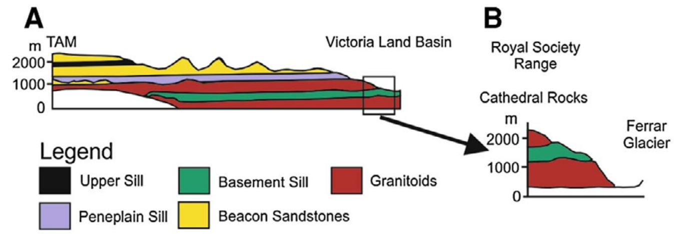

Figure 9. a. Schematic geological cross section from the uplands of the Transantarctic Mountains (TAM) to the Victoria Land Basin (VLB) (Modified after Bédard et al. 2007; Zavala et al. 2011). **b.** Highlight of the Ferrar Glacier area: the Basement sill is located in the upper, inland region of Transantarctic Mountains.

The uppermost interval 4 (770–650 mbsf; 18.7– 17.6 Ma) is characterized by an increase in the Ferrar Group contribution from 750 to 650 mbsf. GHI-Beacon Supergroup, L–M grade metamorphic rocks and carbonates also show an up-core increase. On the contrary, the contribution from the McMurdo Volcanic Group decreases. The presence of McMurdo Volcanic Group mineral assemblages requires ice flow across the Mount Morning volcanic center to the south. Interval 770–750 mbsf displays an up-core increase of the Ferrar Group contribution indicating erosion of dolerites located west of the drill site. As hypothesized by Hauptvogel and Passchier (2012) for their third interval (552–308 mbsf), this would fit a scenario where the grounding lines of outlet glaciers had receded into the valleys of Victoria Land, away from the coast. There, they would have eroded the Ferrar dolerites in the upper section of the Transantarctic Mountains during glacial times with possibly further retreat. Valleys that are eroded into basement rocks near the coast do not reach basement further inland (Denton et al, 1993). In addition, other studies conducted in the McMurdo Sound area by Marsh (2004), Bédard et al. (2007) and Zavala et al. (2011) highlight that there exist four Ferrar sills in the McMurdo Dry Valleys Region of the Transantarctic Mountains. From top to bottom, these are the Mt. Fleming, Asgard, Peneplain and Basement Sills. The upper three sills consist of homogeneous fine- to medium-grained dolerite, whereas the lowermost Basement Sill (Gunn 1962), which extends from McKay Glacier to the head of Ferrar glacier (Figure 9), has a central cumulate layer or ‘tongue’ consisting of large orthopyroxene and smaller plagioclase crystals, enclosed by fine- to medium-grained dolerite like that of the other sills. In the Ferrar Glacier area, the Basement Sill is located inland (Figure 9b), and it is the most likely source for the high amounts of orthopyroxenes.

Ice dynamics and paleoclimatic implications

The AND-2A drill core from Southern McMurdo Sound offers a detailed record of a crucial period in Antarctic climate evolution during the late Early Miocene. The heavy mineral assemblages in Interval 1 indicate that between 20.2 and 20.1 Ma the grounding line of the ice sheet advanced to a position near the present-day Mount Morning volcanic center. However, during deposition of Interval 2 (20.1–19.3 Ma), the ice sheet most likely experienced a dynamic behavior with time interval of ice advance alternating with periods of ice retreat, while Interval 3 (19.3–18.7 Ma) records further retreat to open water conditions. A dynamic behavior is noted in Interval 4 (18.7–17.6 Ma) with a decreasing contribution of materials derived from the basalts of the Mount Morning volcanic center located to the south of the drill site and a consequent increasing contribution of materials derived from Transantarctic Mountains to the west of the drill site.

The clast provenance analysis by Talarico and Sandroni (2011) provided direct evidence of ice sheet expansion in the Ross Embayment during the Early Miocene. The record clearly indicates that the Early Miocene glacial evolution in the McMurdo Sound was closely linked to fluctuations of EAIS outlet glaciers. The unanswered question is whether these fluctuations were accompanied by similar changes in the West Antarctic Ice Sheet. A glacial scenario proposed by Hambrey and Barrett (1993) for the Early Miocene indicates an expansion of EAIS, through amalgamation of all major outlet glaciers, leaving areas located further to the east (i.e., Marie Byrd Land) free of ice.

More recently, Liebrand et al. (2011) presented high-resolution stable isotope records of benthic foraminifera from ODP Site 1264 in the southeastern Atlantic Ocean, in order to resolve the latest Oligocene to Early Miocene climate changes. Their modeling results suggested that during the largest Mi-1 event, Antarctic ice sheet volume expanded to its present-day configuration. They pointed out that major large-scale Antarctic ice sheet expansions coincide with 400 kyr eccentricity minima when the power of the ~100 kyr eccentricity cycle is significantly suppressed (e.g., at ~19.8 Ma). Furthermore, they pointed out that distinct ~100 kyr variability occurs during the termination phases of the major Antarctic glaciations, suggesting that climate and ice sheet response was more susceptible to short-term eccentricity forcing at these times. We are tempted to speculate that the ice sheet buildup phase that they recognized between 20.2–19.8 Ma (Figure 7, p. 876 of Liebrand et al. 2011) roughly coincides with interval 4 of the present study. Interval 3 is characterized by a very dynamic behavior, and this could be related to an interval of ~100 kyr cycle (Liebrand et al. 2011).

Conclusions

The heavy mineral analysis of the lower AND-2A drill core helped to better constrain the timing and the spatial extent of ice growth and decay in the Ross Sea area during the late Early Miocene (17.6–20.2 Ma). On the basis of heavy mineral analysis, the following conclusions can be drawn:

1. The different heavy minerals recognized in the lower 650 mbsf of AND-2A core can be related to six different source rocks.
2. The heavy mineral down-core distribution allowed the identification of four intervals with characteristic assemblages that reflect different source areas.
3. Discriminant function analysis revealed that individual samples can be classified into three predefined groups. Facies associations roughly coincide with the interval subdivision.
4. Interval 3 (19.3–20.1 Ma) recorded for the first time a cyclic Mount Morning volcanic contribution from the south, in combination with fluctuations in L–M grade metamorphic, GHI-Beacon Supergroup and Ferrar Group contributions, which indicated a heavy mineral assemblage derived from a local source.

The results largely confirmed interpretations based on the facies distribution (Passchier et al. 2011) and basement clast provenance (Sandroni and Talarico 2011), and they have added new insight on heavy mineral provenance areas.

Consistent with previous studies (Diekmann and Kuhn 1999; Ehrmann and Polozek 1999; Giorgetti et al. 2009; Hauptvogel and Passchier 2012), the heavy mineral analysis confirms its value to be a powerful tool for the reconstruction of paleo-glacial-flow dynamic and paleogeographic scenarios. The application of such analysis to the Early–Middle Miocene sedimentary interval recovered for the first time by the AND-2A core provides further constraints on the paleogeographic evolution of the southern McMurdo Sound area during Miocene time, showing that the variations of paleoenvironmental drivers characterizing this period were able to exert deep transformation of the Antarctic ice sheet.

We are aware of the fact that our record documents ice buildup and retreat just in one sector of Antarctica and further studies of Early Miocene records from other parts of the Antarctic continental margin will be needed to confirm our conclusions.

Acknowledgments — The ANDRILL Program is a multinational collaboration between the Antarctic programs of Germany, Italy, New Zealand, and the United States. Antarctica New Zealand is the project operator and developed the drilling system in collaboration with Alex Pyne at Victoria University of Wellington and Webster Drilling and Exploration Ltd. Antarctica New Zealand supported the drilling team at Scott Base; Raytheon Polar Services Corporation supported the science team at McMurdo Station and the Crary Science and Engineering Laboratory. The ANDRILL Science Management Office at the University of Nebraska–Lincoln provided science planning and operational support. Scientific studies are jointly supported by the U.S. National Science Foundation (NSF), New Zealand Foundation for Research, Science and Technology (FRST), the Italian Antarctic Research Program (PNRA), the German Research Foundation (DFG), and the Alfred Wegener Institute for Polar and Marine Research (AWI). We are grateful to Dr. Ian Bailey and Dr. Kurt S. Panter for their useful and constructive comments. Dr. Francesco Iacoviello acknowledges the Fundação de Amparo à Pesquisa do Estado de São Paulo (FAPESP) for financial support, Grant Number 2012/18304-3.

References

Acton G, Crampton J, Di Vincenzo G, Fielding CR, Florindo F, Hannah M, Harwood D, Ishman S, Johnson K, Jovane L, Levy R, Lum B, Marcano MC, Mukasa S, Ohneiser C, Olney M, Riesselman C, Sagnotti L, Stefano C, Strada E, Taviani M, Tuzzi E, Verosub KL, Wilson GS, Zattin M, the ANDRILL-SMS Science Team (2008) Preliminary integrated chronostratigraphy of the AND-2A core, ANDRILL Southern McMurdo Sound project, Antarctica. Terra Antarct 15:211–220

ANDRILL SMS Science Team (2010) An integrated age model for the ANDRILL-2A drill core. In: Kontar K, Harwood DM, Florindo F, and Fischbein S (eds) ANDRILL Southern McMurdo Sound project science integration workshop—program and abstracts ANDRILL Contribution # 16, ANDRILL Science Management Office, University of Nebraska, Lincoln, NE, p 113 Armienti P, Messiga B, Vannucci R (1998) Sand provenance from major and trace element analyses of bulk rock and sand grains. Terra Antarct 5:589–599

Barrett P (1979) Proposed drilling in McMurdo Sound: Memoir of the National Institute of Polar Research. Special Issue 13:231–239

Barrett P (2007) Cenozoic climate and sea level history from glacimarine strata off the Victoria Land coast, Cape Roberts Project, Antarctica. In: Hambrey K, Christoffersen P, Glasser N, Hubbart B (eds) Glacial processes and products. Blackwell, New York, pp 259–287

Barrett PJ, Sarti M, Sherwood W (2000) Studies from the Cape Roberts Project, Ross Sea, Antarctica, Initial Reports on CRP-3. Terra Antarct 7:209

Bédard JHJ, Marsh DB, Hersum GT, Naslund HR, Mukasa BS (2007) Large-scale mechanical redistribution of orthopyroxene and plagioclase in the Basement Sill, Ferrar Dolerites, McMurdo Dry Valleys, Antarctica: petrological, mineral-chemical and field evidence for channelized movement of crystals and melt. J Petrol 48:2289–2326

Callahan J (1987) A non-toxic heavy liquid and inexpensive filters for separation of mineral grains. J Sediment Petrol 57:765–766

Cape Roberts Science Team (1998) Initial report on CRP-1, Cape Roberts Project, Antarctica. Terra Antarct 5(1):187

Cook YA, Craw D (2002) Neoproterozoic structural slices in the Ross Orogen, Skelton Glacier area, South Victoria Land, Antarctica. NZ J Geol Geophys 45:133–143

Cooper A, Adam L, Coulter R, Eby G, McIntosh W (2007) Geology, geochronology and geochemistry of a basanitic volcano, White Island, Ross Sea, Antarctica. J Volcanol Geotherm Res 165:189–216

Cramer BS, Miller KG, Barrett PJ, Wright JD (2011) Late Cretaceous– Neogene trends in deep ocean temperature and continental ice volume: reconciling records of benthic foraminiferal geochemistry (δ18O and Mg/Ca) with sea level history. J Geophys Res 116:C12023. doi: 10.1029/2011JC007255

Damiani D, Giorgetti G (2008) Provenance of glacial–marine sediments under the McMurdo/Ross Ice Shelf (Windless Bight, Antarctica): heavy minerals and geochemical data. Palaeogeogr Palaeoclimatol Palaeoecol 260(1–2):262–283. doi: 10.1016/j.palaeo.2007.08.010

Davey FJ, Barrett PJ, Cita MB, van der Meer JJM, Tessensohn F, Thomson MRA, Webb PN, Woolf KJ (2001) Drilling for Antarctic Cenozoic climate and tectonic history at Cape Roberts, Southwestern Ross Sea. Eos Trans Am Geophys Union 82(48):585, 589–590. doi: 10.1029/01EO00339

Denton GH, Sugden DE, Marchant DR, Hal BL, Wilch TI (1993) East Antarctic Ice Sheet sensitivity to Pliocene climatic change from a Dry Valleys perspective. In: A special volume arising from the Vega symposium: the case for a stable east Antarctic ice sheet. Geografiska Annaler Series A, Physical Geography 75(4):155–204

Di Roberto A, Del Carlo P, Rocchi S, Bracciali L, Di Vincenzo G, Rocchi S, Panter K (2012) Early Miocene volcanic activity and paleoenvironment conditions of the AND-2A core (southern McMurdo Sound, Antarctica). Geosphere 8(6):1342. doi: 10.113 0/GES00754.1

Di Roberto A, Giorgetti G, Iacoviello F, Pompilio M (2013) Alteration of volcanic deposits in the ANDRILL AND-1B core: influence of paleodeposition, eruptive style, and magmatic composition. Geosphere 9:1–12. doi: 10.1130/GES00812.1

Di Vincenzo G, Bracciali L, Del Carlo P, Panter K, Rocchi S (2010) 40Ar–39Ar dating of volcanogenic products from the AND-2A core (ANDRILL Southern McMurdo Sound Project, Antarctica): correlations with the Erebus Volcanic Province and implications for the age model of the core. Bull Volcanol 72:487–505

Diekmann B, Kuhn G (1999) Provenance and dispersal of glacial– marine surface sediments in the Weddell Sea and adjoining areas, Antarctica: ice-rafting versus current transport. Mar Geol 158:209–231

Dill HG (1998) A review of heavy minerals in clastic sediments with case studies from the alluvial-fan through the nearshore-marine environments. Earth Sci Rev 45:103–132

Dreimanis A, Vagners UJ (1972) The effect of lithology upon texture of till. In: Yatsu E, Falconer A (eds) Research methods in Pleistocene geology: 2nd Guelph symposium geomorphology, pp 66–82

Dunbar NW, Panter K, Scanlan MK, Fargo A, McIntosh WC, Wilch TI (2008) Evidence for complex mixing processes controlling the composition of a wide range of alkaline volcanic rocks at Minna Bluff, Antarctica. American Geophysical Union Fall 2008 Meeting, Abstract V13C-2128

Ehrmann WU, Polozek K (1999) The heavy mineral record in the Pliocene to Quaternary sediments of the CIROS-2 drill core, McMurdo Sound, Antarctica. Sediment Geol 128:223–244

Elliott DH (1992) Jurassic magmatism and tectonism associated with Gondwanaland break-up: an Antarctic perspective. In: Storey BC, Alabaster T Punkhurst RJ (eds) Magmatism and the causes of continental break-up. London, Geological Society, London, Special Publication 68, pp 165–184

Fahnestock MA, Scambos TA, Bindschadler RA, Kvaran G (2000) A millennium of variable ice flow recorded by the Ross Ice Shelf, Antarctica. J Glaciol 46:652–664

Fielding CR, Thomson MRA (1999) Studies from the Cape Roberts Project, Ross Sea Antarctica, initial report on CRP-2/2A. Terra Antarctica, Bremerhaven, PANGAEA, 6(1), pp 173

Fielding CR, Henrys SA, Wilson TJ (2006) Rift history of the western Victoria Land Basin: a new perspective based on integration of cores with seismic reflection data. In: Fütterer D, Damaske D, Kleinschmidt G, Miller H, Tessensohn F (eds) Antarctica contributions to global earth sciences. Springer, Berlin, pp 309–318

Fielding C, Atkins C, Bassett K, Browne G, Dunbar G, Field B, Frank T, Krissek L, Panter K, Passchier S, Pekar S, Sandroni S, Talarico F, the ANDRILL-SMS Science Team (2008a) Sedimentology and stratigraphy of the AND-2A Core, ANDRILL Southern McMurdo Sound Project, Antarctica. Terra Antarct 15:77–112

Fielding CR, Whittaker J, Henrys SA, Wilson TJ, Naish TR (2008b) Seismic facies and stratigraphy of the Cenozoic succession in McMurdo Sound, Antarctica: implications for tectonic, climate and glacial history. Palaeogeogr Palaeocl 260:8–29. doi: 10.1016/j.palaeo.2007.08.016

Fitzgerald P (1992) The Transantarctic Mountains of southern Victoria Land: the application of apatite fission track analysis to a rift shoulder uplift. Tectonics 11(3):634–662

Fitzgerald P (2002) Tectonics and landscape evolution of the Antarctic plate since the breakup of Gondwana, with an emphasis on the West Antarctic Rift System and the Transantarctic Mountains. In: Gamble JA, Skinner DNB Henrys S (eds) Antarctica at the close of a millennium: Royal Society of New Zealand Bulletin, vol 35, pp 453–469

Florindo F, Harwood DM, Talarico F, Levy RH, the ANDRILL-SMS Science Team (2008) ANDRILL Southern McMurdo Sound Project, Antarctica. In: Harwood DM, Florindo F, Talarico F, Levy RH (eds) Studies from the ANDRILL, Southern McMurdo Sound Project, Antarctica. Terra Antarctica, vol 15, pp 13–20

Gamble JA, Barrett PJ, Adams CJ (1986) Basaltic clasts from Unit 8. In: Barrett PJ (eds) Antarctic Cenozoic History from the MSSTS-1 Drillhole, McMurdo Sound. DSIR Bull 237:145–152

George A (1989) Sand provenance. In: Barrett PJ (eds) Antarctic Cenozoic History from the MSSTS-1 Drillhole, McMurdo Sound. DSIR Bull 237:159–167

Ghent ED, Henderson RA (1968) Geology of the Mt. Falconer Pluton, lower Taylor Valley, South Victoria Land, Antarctica. NZ J Geol Geophys 11(4):851–879

Giorgetti G, Talarico F, Sandroni S, Zeoli A (2009) Provenance of Pleistocene sediments in the ANDRILL AND-1B drillcore: clay and heavy mineral data. Global Planet Change 69:94–102

Goodge JW (2007) Metamorphism in the Ross Orogen and its bearing on Gondwana margin tectonics. In Cloos M, Carlson WD, Gilbert MC, Liou JG and Sorensen SS (eds) Convergent Margin Tectonics and Associated Regions: a tribute to WG Ernst, Geological Society of America Special Paper 419, pp 185–203

Goodge JW, Williams IS, Myrow P (2004) Provenance of Neoproterozoic and lower Paleozoic siliciclastic rocks of the central Ross orogen, Antarctica: detrital record of rift-, passive- and activemargin sedimentation. Geol Soc Am Bull 116:1253–1279

Gunn BM (1962) Differentiation in Ferrar Dolerites. NZ J Geol Geophys 5(5):820–863

Gunn BM, Warren G (1962) Geology of Victoria Land between the Mawson and Mulock Glaciers, Antarctica. NZ Geol Surv Bull 71:1–157

Gwyn QHJ, Dreimanis A (1979) Heavy mineral assemblages in tills and their use in distinguishing glacial lobes in the Great Lakes region. Can J Earth Sci 16:2219–2235

Haban MA, Elliot DH (1985) Mineral chemistry of the Kirkpatrick basalt, northern Victoria Land. Antarct J Unit States 19:30–31

Hambrey MJ, Barrett PJ (1993) Cenozoic sedimentary and climatic record, Ross Sea region, Antarctica. In: Kennett JP, Warnke DA (eds) The Antarctic paleoenvironment: a perspective on global change. Antarctic Research Series, vol 60, pp 91–124

Hanan MA, Totten MW (1996) Analytical techniques for the separation and SEM identification of heavy minerals in mudrocks. J Sediment Res 66:1027–1030

Harwood DM, Florindo F, Talarico F, Levy RH (eds) (2008) Studies from the ANDRILL, Southern McMurdo Sound Project, Antarctica. Terra Antarctica, vol 15, pp 253

Harwood DM, Florindo F, Talarico FM, Levy RH, Kuhn G, Naish T, Niessen F, Powell R, Pyne A, Wilson G (2009) Antarctic drilling recovers stratigraphic records from the continental margin. Eos 90:90–91

Hauptvogel DW, Passchier S (2012) Early-Middle Miocene (17– 14 Ma) Antarctic ice dynamics reconstructed from the heavy mineral provenance in the AND-2A drill core, Ross Sea, Antarctica. Global Planet Change 82–83:38–50

Iacoviello F, Giorgetti G, Nieto F, Memmi IT (2012) Evolution with depth from detrital to authigenic smectites in sediments from AND-2A drill core (McMurdo Sound, Antarctica). Clay Miner 47:481–498. doi: 10.1180/claymin.2012.047.4.07

Kominz MA, Browning JV, Miller KG, Sugarman PJ, Misintzeva S, Scotese CR (2008) Late Cretaceous to Miocene sea-level estimates from the New Jersey and Delaware coastal plain coreholes: an error analysis. Basin Res 20:211–226

Kyle PR (1990) McMurdo Volcanic Group, western Ross embayment. Introduction. In: Le Masurier WE, Thomson JW (eds) Volcanoes of the Antarctic plate and Southern Oceans. AGU Antarctic Research Series, vol 48, pp 19–25

Kyle P, Moore J, Thirlwall M (1992) Petrologic evolution of anorthoclase phonolite lavas at Mount Erebus, Ross Island, Antarctica. J Petrol 33:849–875

La Prade KE (1982) Petrology and petrography of the Beacon Supergroup, Shackleton Glacier area, Queen Maud Range, Transantarctic Mountains, Antarctica. In: Proceedings of the third symposium on Antarctic geology and geophysics. The University of Wisconsin Press, Madison, Wisconsin, USA, pp 581–590

Laird MG, Bradshaw JD (1982) Uppermost proterozoic and lower paleozoic geology of the Transantarctic mountains. In: Craddock C (ed) Antarctic geoscience. University Wisconsin Press, Madison, pp 525–533

LeMasurier WE, Thomson JW (eds) (1990) Volcanoes of the Antarctic Plate and Southern Oceans, Antarctic Research Series, vol 48, pp 488

Licht KJ, Lederer JR, Swope J (2005) Provenance of LGM glacial till (sand fraction) across the Ross embayment, Antarctica. Quat Sci Rev 24:1499–1520

Liebrand D, Lourens LJ, Hodell DA, de Boer B, van de Wal RSW, Pälike H (2011) Antarctic ice sheet and oceanographic response to eccentricity forcing during the early Miocene. Clim Past 7:869–880. doi: 10.5194/cp-7-869-2011

Lopatin BG (1972) Basement complex of the McMurdo 'oasis', southern Victoria Land. In: Adie RJ (ed) Antarctic geology and geophysics. Universitetsforlaget, Oslo, pp 287–292

Marsh BD (2004) A magmatic mush column Rosetta Stone: the McMurdo dry valleys of Antractica. EOS Trans Am Geophys Union 85:497–502

Martin AP (2009) Mt. Morning, Antarctica: Geochemistry, geochronology, petrology, volcanology, and oxygen fugacity of the rifted Antarctic lithosphere. Ph.D. thesis, Dunedin, University of Otago

Martin AP, Cooper AF, Dunlap WJ (2010) Geochronology of Mount Morning, Antarctica: two-phase evolution of a longlived trachyte–basanite–phonolite eruptive center. Bull Volcanol 72:357–371

McKelvey BC, Webb PN, Kohn BP (1977) Stratigraphy of the Taylor and lower Victoria Groups (Beacon Supergroup) between Mackay Glacier and Boomerang range, Antarctica. NZ J Geol Geophys 20:813–863

Morton AC (1985) Heavy-minerals in provenience studies. In: Zuffa GG (ed) Provenance of arenites. NATO ASI, Ser. C, vol 148, pp 249–277

Morton AC, Hallsworth CR (1999) Processes controlling the composition of heavy mineral assemblages in sandstones. Sediment Geol 124(1–4):3–29

Naish T, Powell R, Levy RH (eds) (2007) Studies from the ANDRILL, McMurdo Ice Shelf Project, Antarctica. Initial Science Report on AND-1B. Terra Antarctica vol 14, pp 328

Neumann M (2001) Preliminary investigations of heavy mineral record from CRP-3 Drillcore, Victoria Land Basin, Antarctica. Terra Antart 8:517–522

Nyland RE, Panter KS, Rocchi S, Di Vincenzo G, Del Carlo P, Tiepolo M, Field B, Gorsevski P (2013) Volcanic activity and its link to glaciation cycles: single-grain age and geochemistry of Early Miocene volcanic glass from ANDRILL AND-2A core, Antarctica. J Volcanol Geotherm Res 250:106–128

Okay N, Ergün B (2005) Source of the basinal sediments in the Marmara Sea investigated using heavy minerals in the modern beach sands. Mar Geol 216:1–15

Panter KS, Talarico F, Bassett K, Del Carlo P, Field B, Frank T, Hoffmann S, Kuhn G, Reichelt L, Sandroni S, Taviani M, Bracciali L, Cornamusini G, von Eynatten H, Rocchi S, the ANDRILL-SMS Science Team (2008) Petrologic and geochemical composition of the AND-2A Core, ANDRILL Southern McMurdo Sound Project, Antarctica. Terra Antart 15:147–192

Panter KS, Dunbar, N, Scanlan M, Wilch T, Fargo A, McIntosh W (2011) Petrogenesis of alkaline magmas at Minna Bluff, Antarctica: evidence for multi-stage differentiation and complex mixing processes. Abstract V31f-2590 presented at the 2011 Fall Meeting, AGU, San Francisco, CA, USA, 5–9 Dec

Passchier S (2001) Provenance of the Sirius Group and related Upper Cenozoic glacial deposits from the Transantarctic Mountains, Antarctica: relation to landscape evolution and ice-sheet drainage. Sediment Geol 144(3–4):263–290

Passchier S (2007) Chapter 27, the use of heavy minerals in the reconstruction of ice-sheet drainage patterns: an example from the edge of the east antarctic ice sheet. Developments in Sedimentology, vol 58, pp 677–699. ISSN: 0070-4571. doi: 10.1016/ S0070-4571(07)58027-1

Passchier S, Browne G, Field B, Fielding CR, Krissek LA, Panter K, Pekar SF, ANDRILL-SMS Science Team (2011) Early and Middle Miocene Antarctic glacial history from the sedimentary facies distribution in AND-2A drill hole, Ross Sea, Antarctica. Geol Soc Am Bull 123(11/12):2352–2365

Paulsen T, Encarnación J, Valencia VA, Roti Roti J, Rasoazanamparany C (2011) Detrital U-Pb zircon analysis of an Eocene McMurdo Erratic sandstone, McMurdo Sound, Antarctica. NZ J Geol Geophys 54:354–360

Polozek K (2000) Distribution of heavy minerals in CRP-2/2A, Victoria land Basin, Antarctica. Terra Antarct 7:567–573

Polozek K, Ehrmann W (1998) Distribution of heavy minerals in CRP-1. Terra Antarct 5(3):633–638

Pompilio M, Kyle P, Wilch T, Dunbar N, ANDRILL-MIS Project Science Team (2007) The volcanic record in the ANDRILL McMurdo Ice Shelf AND-1B drill core. U.S. Geological Survey and The National Academies; USGS OF-2007-1047, Extended Abstract 199, 10th international symposium on Antarctic sciences, ANDRILL Research and Publications, Paper 4

Rimington N, Cramp A, Morton A (2000) Amazon fan sands: implications for provenience. Mar Pet Geol 17:267–284

Sandroni S, Talarico F (2004) Petrography and provenance of basement clasts in CIROS-1 core, McMurdo Sound, Antarctica. Terra Antarct 11:93–114

Sandroni S, Talarico F (2011) The record of Miocene climatic events in AND-2A drill core (Antarctica): insights from provenance analyses of basement clasts. Global Planet Change 75:31–46

Skinner DNB (1982) Stratigraphy and structure of lower grade metasediments of Skelton Group, McMurdo Sound: does Teall Greywacke really exist? In: Craddock C (ed) Antarctic geoscience. University of Wisconsin Press, Madison, pp 555–563

Smellie JL (2000) Erosional history of the Transantarctic Mountains deduced from sand grain detrital modes in CRP-2/2A, Victoria Land Basin, Antarctica. Terra Antarct 7:545–552

Smillie RW (1992) Suite subdivision and petrological evolution of granitoids from the Taylor Valley and Ferrar Glacier region, south Victoria Land. Antarct Sci 4:71–87

Stump E (1995) The Ross Orogen of the Transantarctic Mountains. Cambridge University Press, Cambridge

Stump E, Gootee BF, Talarico F, Van Schmus WR, Brand PK, Foland KA, Fanning CM (2004) Correlation of Byrd and Selborne Groups, with implications for the Byrd Glacier discontinuity, central Transantarctic Mountains. NZ J Geol Geophys 47:157–171

Stump E, Gootee BF, Talarico F (2006) Tectonic model for development of the Byrd Glacier discontinuity and surrounding regions of the Transantarctic Mountains during the Neoproterozoic—Early Paleozoic. In: Fütterer DK, Damaske D, Kleinschmidt G, Miller H, Tessensohn F (eds) Antarctica: Contributions to global earth sciences. Springer, Berlin, Heidelberg, New York, pp 181–190. doi: 10.1007/3-540-32934-X_22

Talarico FM, Sandroni S (2011) Early Miocene basement clasts in ANDRILL AND-2A core and their implications for paleoenvironmental changes in the McMurdo Sound region (western Ross Sea, Antarctica). Global Planet Change 78(1–2):23–35

Warren G (1969) Geology of the Terra Nova Bay-McMurdo Sound area, Victoria Land. Antarctic Map Folio Series 12, Geology, Sheet 14, American Geographical Society, New York

Wilson TJ (1999) Cenozoic structural segmentation of the Transantarctic rift flank in southern Victoria Land. Global Planet Change 23:105–127

Wilson GS, Roberts AP, Verosub KL, Florindo F, Sagnotti L (1998) Magnetobiostratigraphic chronology of the Eocene-Oligocene transition in the CIROS-1 core, Victoria Land margin, Antarctica: implications for Antarctic glacial history. Geol Soc Am Bull 110:35–47

Wong FL (2002) Heavy mineral provinces of the Palos Verdes margin, southern California. Cont Shelf Res 22:899–910

Zattin M, Andreucci B, Thomson SN, Reiners PT, Talarico FM (2012) New constraints on the provenance of the ANDRILL AND-2A succession (western Ross Sea, Antarctica) from apatite triple dating. Geochem Geophys Geosyst 13:Q10016. doi: 10.1029/201 2GC004357

Zavala K, Leitch AM, Fisher GW (2011) Silicic segregations of the Ferrar Dolerite sills, Antarctica. J Petrol 52(10):1927–1964